IEA TASK I SUBTASK E

VALIDATION OF THE SVS SOLAR HEATING SYSTEM SIMULATION CODE

BY

PEDER VEJSIG PEDERSEN

AND

OVE JØRGENSEN

THERMAL INSULATION LABORATORY

TECHNICAL UNIVERSITY OF DENMARK

SEPTEMBER 1979

REPORT NO 95

Table of contents

Summary

The solar heating system at the Los Alamos National Security and Resources Study Center was calculated for two 14-days periods (in February and December, 1978) with the Danish solar system simulation code, SVS, and the results compared to the measured data. These comparisons are presented in tables and curves in chapter 2.

Before the calculation on the second period the SVS-program was improved by modelling more realistically the pump control and the piping heat losses. However, the collector subroutine was not improved at the same time - this resulted in larger differences for the second period than for the first, because a too high collector output had been outbalanced by too big piping heat losses in the simulation on the first period.

Because of this the validation of the program was concentrated on improving the collector subroutine. This process is described in chapter 3. The calculation of the collector output was reduced considerably by introducing collector heat capacity in the model and by improving the calculation of the convection losses.

Chapter 4 contains the final comparisons between measured and simulated values for the December period. The agreement is excellent on the primary circuit, but less fine on the secondary side. An explanation of discrepancies is also attempted in chapter 4.

INTRODUCTION

The work presented in this report is part of the energy research activities which are done by the participant countries of the International Energy Agency (IEA). Solar Heating and Cooling was one of the technologies selected by the IEA for a collaborative effort, and several projects or "tasks" were initiated. "Investigation of the performance of Solar Heating and Cooling Systems" is Task I in the programme, one of the subtasks of Task I is: Validation of simulation programs. This report presents work carried out under this subtask by the Danish participants. It was decided to make the first validation work with a calculation on the U.S. National Security and Resources Study Center solar heating system in Los Alamos. The participants received data of the solar system and measured data for two periods from Jim Hedstrom, Los Alamos Scientific Laboratory.

A summary report presenting the work on these data of all participants will be due in early 1980.

CHAPTER I

THE DATA AND THE PROGRAM

1.1 Description of the Los Alamos Study Center solar heating system.

The Study Center is located in Los Alamos, N.M. which has a latitude of 35.8° and a longitude of 106°. Here the LASL solar energy group has developed a solar heating and air conditioning system, with a nominal collector area of 743 m^2.

The validation work is done on the solar heating system for two winter periods of 14 days each. 1/2 - 14/2, 78 and 18/12 - 31/12, 78.

For the February-period, it was reported from Los Alamos that the storage losses were much higher than earlier experiments had shown. The explanation of this was that it apparently was due to thermosyphoning and expansion into the cooling system pipings. An increase of 4 or 5 times the original loss coefficients, it was reported, would be appropriate for this period. For the December-period the storage losses were reported to be normal.

In the December period there was no domestic hot water load because the DHW-loop was valved off.

The data are measured with an accuracy of less than 10%.

Fig. 1

The measured heat flows in the solar heating system:

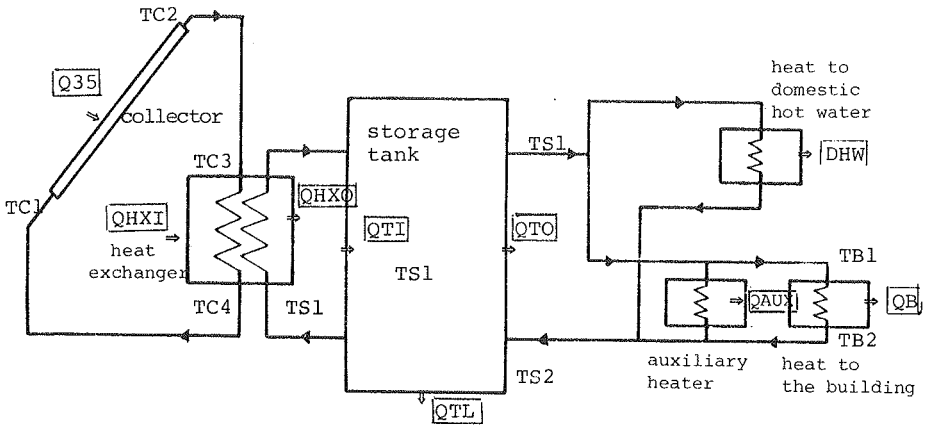

Q is heat

T is temperature, (only temperatures used in the SVS-simulation is shown)

The measured data from Study Center

DATE	MONTH	
DATE	DAY	
TIME	HOUR	
QH	Horizontal Insolation	kW
Q35	35^{o} Insolation	kW
TA	Ambient Temperature	^{o}C
WV	Wind Velocity	m/s
DIR	Wind Direction (N-O, E-90)	Deg
QB	Building Load (w3 * C * (T9-T10))	kW
DHW	DHW Load (W4 * C * (T13-T14)	kW
MODE	1 - Solar, 2 Auxiliary	
QHXI	Heat Exchanger Input (W1 * C * (T1-T2)	kW
QHXO	Heat Exchanger Output (W2 * C * (T3-T4)	kW
QTI	Tank Input (W2 * C * (T5-T6)	kW
QTO	Tank Output (W3 * C * (T7-T8)	kW
QAUX	Auxiliary Output (W3 * C * (T11-T12)	kW
TSAV	Average Tank Temperature	^{o}C

- Temperatures and mass flows here are given in fig (1) in appendix B.
- All heat flows are integrals over the previous hour. (15 sec. samples rate).
- TA, WV, DIR, MODE, TSAV are instanteneous values at the hour.
- Q35, TA, QB, DHW and WV are used as input for the simulation in the SVS-program.

Control of collector and heating of building

I. Collector

1. Differential temperature controller works between absorber surface temperature and tank temperature
2. ON $\Delta T \geq 10^{o}F$ ($5.6\ ^{o}C$)
3. OFF $\Delta T \leq 0^{o}F$ ($0\ ^{o}C$)

II. Heating of building

a. Mode 1 Solar heat
Mode 2 Auxiliary heat

b. Switchover temperature: when the storage temperature is below a set temperature T_s, which is a function of T_a, then switch to auxiliary:

	February	December
Mode 1 → 2	$T_s \leq 39.97-.558\ T_a$	$T_s \leq 39.2-.7\ T$
Mode 2 → 1	$T_s \geq 40.64-.558\ T_a$	$T_s \geq 40.4-.7\ Ta$

temperatures in ^{o}C

Measured Collector Performance

Side-by-side collector test of the LASL STUDY CENTER COLLECTORS 20.01.77 - 06.03.77.

$F_R * \tau\alpha = 0.810$

$F_R * U_L = 4.962\ W/m^2\ ^{o}C.$

Then the efficiency is:

$$\eta = F_R * (\tau\alpha - U_L(TC1 - T_a)/Q35)$$

$$= 0.810 - 4.962 \frac{(TC1 - T_a)}{Q35}$$

1.2 The simulation of the solar heating system by the SVS-program

The SVS (SolVarmeSystem) solar heating simulation program is developed at the Thermal Insulation Laboratory at the Technical University of Denmark.

The program consists of a number of subroutines, which each either model components or have mathematical functions. The program is quasi-stationary, meaning that the enery flows within the time steps are supposed to be stationary.

A control routine for the energy flows has to be programmed for each system to be simulated. When a whole year is calculated, the program continues month by month until the same mean storage temperature is obtained. In this way the start up effect is avoided.

Simulation results

Fig. 2. The calculated heat flows and temperatures in the SVS-program:

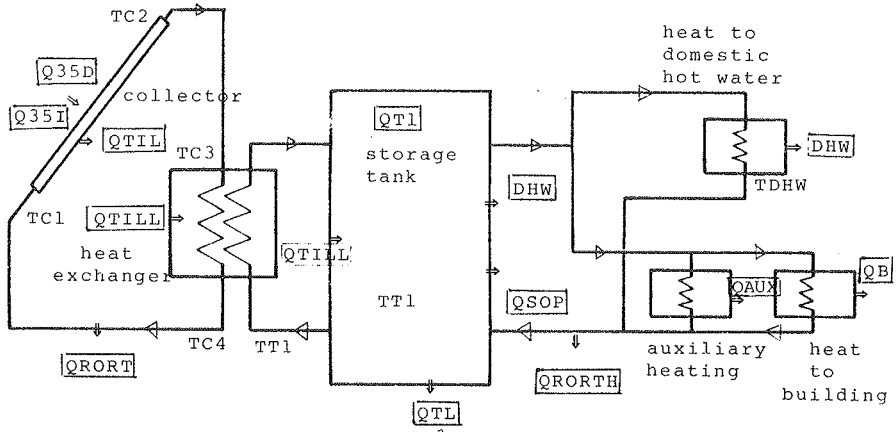

The simulation of the solar heating system yields the following results:

Q35D = Q35 x 0.75 x SFAK	direct 35° insolation	(kW)
Q35I = Q35 x 0.25	diffuse 35° insulation	(kW)
QSOL	collector output predicted on tank temperature	(kW)
QTIL = QSOL x F'''	collector output taking heat exchanger into account	(kW)
QRORT	heat loss from pipes in collector circuit	(kW)
QTILL = QHXI = QHXO = QTI = (QTIL - QRORT)	solar heat to storage (the heat to storage is assumed to be the same as the heat to the heat exchanger)	(kW)
QTL	tank loss	(kW)
QRORTH	heat loss from pipes in heating circuit	(kW)
QSOP = QB (mode 1); 0 (mode 2)	solar energy for building heating	(kW)
QT1 = QT1-QTL-QRORTH-DHW-QSOP	heat in the storage tank	(kW)
TT1 = TSAV = QT1/HCST	storage tank temperature	(°C)

HCST = Heat capacity of storage tank

Calculation of the solar heating system by the SVS-program

Data of the solar heating system

Collector circuit:

Solar collector fluid:	Shell Thermia 33
specific heat, $C_{p,s}$	1970 J/kg ^{o}Cm (at 50 ^{o}C)
density, ρ_s	857.5 kg/m^3 (- " -)
Pump:	Taco Model No 5010
flow rate, $\dot{m}_s$	(0.908*TC4-0.0064*TC4^2-2.82)*3600 kg/h

Piping:

heat loss,	0.1 W/m^2_c ^{o}C
heat capacity	5 kJ/m^2_c ^{o}C
heat loss to	21.1 ^{o}C

Heat exchanger circuit:

Flow rate, $\dot{m}_{vv}$	19.85*3600 (kg/h)
Fluid	water
heat capacity, $C_{p,v}$	4180. J/kg ^{o}C (at 50 ^{o}C)
density, ρ_v	988. kg/m^3 (- " -)

We do not take into account heat loss from the heat exchanger and the heat exchanger circuit leading to the storage tank. These losses are considered to be low compared to other losses in the system.

Heat Exchanger Model B & G 2010-46

Heat exchanger type Tube in Shell.

Measured heat tranfer coefficient, U_H = 12521 + 282*(TC4), $(W/^{O}C)$

= QTILL/(TC4-TS1)

We use a regression analysis on the below listed equations to find the heat exchanger factor, F''', and the heat exchange efficiency ϵ_{vv}.

$$\epsilon_{vv} = \frac{TC3-TC4}{TC3-TS1} = \frac{(1-\exp(-NTU*(1-\kappa))}{(1-\exp(-NTU*(1-\kappa)))}$$

$$NTU = \frac{U_H}{\dot{m}_s * C_{p,s}} \quad , \quad \kappa = \frac{\dot{m}_s * C_{p,s}}{\dot{m}_{vv} * C_{p,v}}$$

$$F''' = \left[1 + \left(\frac{U_L * F' * F''}{\dot{m}_s \cdot C_{p,s}}\right) * \left(\frac{1}{\epsilon_{vv}} - 1\right)\right]^{-1}$$

Here we use U_L = 4.0 $W/m^2\ ^{o}C$

F' = 0.98, F'' = 0.97

We calculate F''' and ϵ_{vv} for different values of, TC4, and find ϵ_{vv} to be 0.370 ± 0.010.

As a result of the calculation we use ϵ_{vv} = 0.37 and and F''' = 0.92.

The reason why it is necessary to use constant values for F''' and ϵ_{vv} in the program, is that F''' is a function of $\dot{m}_s$. But it is also true that $\dot{m}$ is a function of TC4, which is a function of F'''. This means that the alternative would be to make an iteration process in the program.

Storage tank

fluid:	water	
volume:	37.85 m^3	
insulation:	fiberglass	
thickness		51 mm
conductivity		0.36 $W/m\ ^oC$
calculated loss		0.71 $W/m^2\ ^oC$
measured loss, (used) $U_{L,S}$		0.64 $W/m^2\ ^oC$
heat loss to		21.1 ^oC
start temperature in February		39.2 ^oC
start temperature in December		41.2 ^oC

Stratification is not taken into account.

Domestic hot water circuit

Flow rate, $\dot{m}_{dv}$ 0.95 kg/s

In the Study Center system there is no back up on domestic hot water.

Heat exchange in domestic hot water tank

We use a U_{DHW}-value of 2035 $W/^oC$.
Then the efficiency ϵ_{dv} is calculated as:

$$\epsilon_{dv} = 1 - \exp\left(\frac{-U_{DHW}}{\dot{m}_{dv}}\right)$$

Building heating circuit:

fluid:	water
flow rate, $\dot{m}_{bv}$	3.78 kg/s
pipe length	40 m
heat loss	0.15 $W/m_{bv}\ ^oC$
heat capacity	2.16 $kJ/m_{bv}\ ^oC$
heat loss to	21.1 ^oC

NB. A detailed description of the simulation of the solar heating system by the SVS program is given in Appendix A.2.

Calculation of the solar collector in the SVS-program

Data of the solar collector used in the SVS-program

Aperture are	715.8 m^2
Tilt	35^o
Direction	13^o east of south
Glazing	1 sheet ASG white glass
measured transmission, τg	0.91
thickness, E	3.175 mm
extension coefficient, K	0.024 cm^{-1}
refractive index for glass, n	1.526
Absorber	seam welded expanded steel
surface	black chrome
absorptivity, α	0.93
emissivity, ε_p	0.09
Back insulation	urethane foam
thickness, D_b	50.8 mm
conductivity, λ_b	0.0288 W/m ^oC
heat loss to	21.1 ^oC

Side and end heat loss will be calculated as 5% of the front heat loss.

Shade factors (SFAK):

Time	7	8	9	10	11	12	13	14	15	16	17
February	.907	.949	.964	.974	.978	1.0	1.0	.969	.899	.781	.763
December	1.0	.948	.972	.972	.979	1.0	.997	.944	.841	.749	1.0

NB. The collector subroutine of the SVS-program is presented in appendix A.3. Here you can find all relevant equations and parameters. Most of the equations used in this subroutine is from reference [2].

A detailed description of the simulation of the solar heating system by the SVS program is given in Appendix A.2.

CHAPTER II

THE FIRST COMPARISONS

2.1 February comparisons

Original SVS program compared to February data

The results of the calculation of the February period using the original SVS-program are compared to the measured values in fig. 1 to 3 on the following pages.

As expected, (see paragraph 1.1) we got the best agreement when using a five times greater tank heat loss than given. In this case the calculated value of QTO is only 349 kWh (2.9%) higher than the measured QTO (see table 1). In figure 1 and 2 we have plotted the calculated and the measured tank temperature TSAV, and here you find a good agreement between calculated and measured values when the five times greater tank loss is taken into account. (The calculated TSAV is 0-5 ^{o}C higher than the measured TSAV).

Because of the uncertainty of how big the tank losses really were, it was difficult to use the February run to make validation work on the SVS-program. Thus we decided to do this with the next run, with new data from December 78, where the problems with the tank heat losses had disappeared.

Table 1.

Comparisons of the SVS-results to the data from Los Alamos, Study Center

3: Measured 14 days summary of results:

2: SVS-results for 5 times greater tank heat loss than given

1: SVS-results for the tank heat loss given:

			1 (kWh)	2 (kWh)	3 (kWh)
A	35^{O} insolation (reduced)	Q35R	44,765	44,765	Q35= 46,509
B	Absorbed solar		17,437	16,644	
C	Storage Tank Heat Loss		667	2,966	2,714
D	Building Load	QB	17,273	17,273	17,273
E	Solar Heat to the Building		13,447	11,908	11.510
F	Auxiliary Output	QAUX	3,837	5,381	5,382
G	DHW Load	DHW	300	300	333
H	Solar Heat to DHW		289	284	333
I	% Solar of DHW		97	95	100
J	Total Load	D+G	17,573	17,573	17,606
K	Tank Output	QTO	13,736	12,192	11,843
L	Fraction of Load carried by Solar %	$\frac{D+G-QAUX}{D+G}$	77	69	69.4

Fig. 1. Measured and calculated tank temperatures (tank loss 5x)

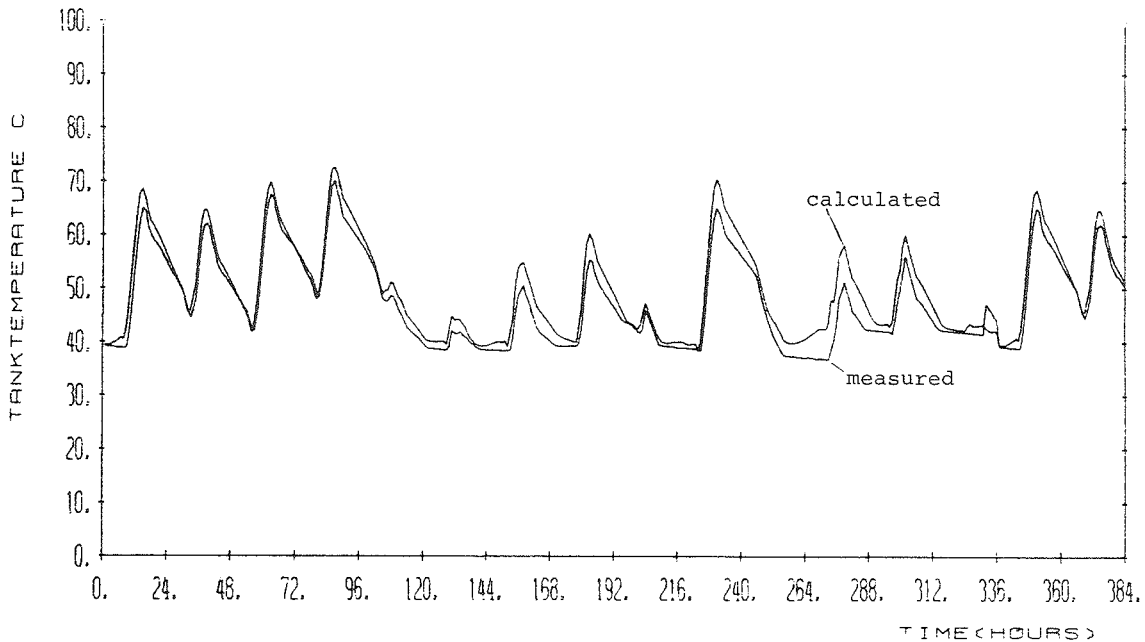

Fig. 2. Measured and calculated tank temperatures (tank los lx)

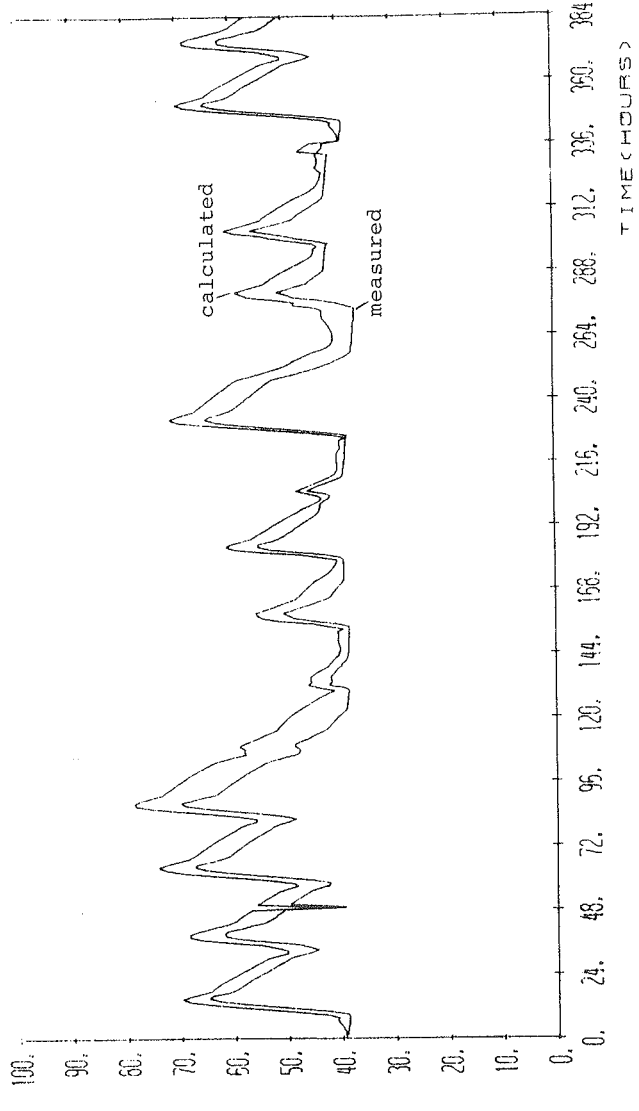

New version of the SVS-program compared to February data

When starting the work on the December data, we were in some sort of a dilemma. The problem was that, in the meantime, we has improved the SVS-program. This meant that now it was possible to use a new and better way to control the pump in the collector circuit, and, furthermore, a new and more realistic way of calculating pipe heat losses was introduced. These changes resulted in higher efficiency of the solar system than before because the previous too positive predictions of the collector subroutine were balanced out by the piping losses.

In our opinion, the goal of the validation work is to improve the simulation programs. Therefore we decided to use the new SVS-version (SVS(N)) for the December comparisons, being aware of the fact that it would give too high results. And then later, when we had time, we improved the collector routine by using the December data.

The differences of the results for the February period between the two SVS-versions is seen in the table 2, next page. As you see, QHXI is 1013 kWh higher in the last and changed version. This is an increase of 8%.

Comparison between the original SVS-version SVS(O) and the new version SVS(N), when calculating the Study Center solar heating system with February data (14 days.

Table 2.

(kWh)	Measured	SVS(O)	SVS(N)
QSUN	46509	46509	46509
QCOLL		16786	17054
QHXI	14370	15193	16206
QTL		3001	2974
QTO	11843	12192	13158
QB	17434	17434	17434
QAUX	5382	5245	4279

The first run with December-78 data is called the SVS(1) run. The results are presented in the next paragraph.

2.2 December comparisons

Presentation of the SVS-results from the first run with December 78 data, SVS(1).

The input data for the period are given in the table below:

Table 3

	INPUT QUANTITIES			
DAY	QSUN (KWH)	QB (KWH)	TA (C)	WV (M/S)
18	654.0	1705.0	1.7	1.5
19	2320.0	1504.5	2.9	4.2
20	4500.0	1915.4	-4.7	2.8
21	4323.0	1877.2	-5.0	0.5
22	4381.0	1811.4	-3.4	0.3
23	4498.0	1845.8	-3.4	2.4
24	4353.0	1984.8	-3.6	0.6
25	4355.0	1824.4	-0.3	0.7
26	4464.0	1806.7	-2.8	1.0
27	4182.0	1749.7	-1.5	0.5
28	1582.0	1547.2	1.2	3.6
29	2735.0	1510.4	1.2	2.6
30	517.0	1839.2	-0.5	0.7
31	1928.0	1795.4	-2.9	1.1
TOTAL	44792.0	24717.1	-1.5	1.6

We have tried to present the results of this run in a way like that proposed by W.J. Kennish [7]. We use three different tables and four figures:

table 4: Comparison of predicted and measured performance values.

table 5: Comparison of predicted and measured values of QHXI, QTO and QAUX and differences and standard deviation.

Figure 3: Solar heat to heat exchanger, QHXI, measured and predicted, day 19 and 20.

figure 4: Solar heat to heat exchanger, QHXI, measured and predicted, day 21 and 22.

figure 5: tank temperature, TSAV, measured and predicted, day 19 and 20.

figure 6: tank temperature, TSAV, measured and predicted, day 21 and 22.

In the tables 4 to 5 we make comparisons between dayly results and results for the whole period. While in the figures 3 to 6 the results are compared on an hourly basis.

Presentation of the SVS(1) run on the Study Center solar heating system with December 78 data.

Table 4.

PERFORMANCE VALUES

predicted vs. measured

DAY	QSUN (kWh)	⌜collector output⌝ $QHXI_p$ (kWh)	$QHXI_m$ (kWh)	EFF_p (%)	EFF_m (%)	F_p (%)	F_m (%)
18	654.0	0.0	0.0	0.0	0.0	18.4	7.6
19	2320.0	959.8	775.0	42.4	33.4	44.9	46.3
20	4500.0	1723.1	1566.0	40.0	34.8	66.2	61.3
21	4323.0	1653.7	1523.0	40.0	35.2	83.0	69.3
22	4381.0	1708.8	1666.0	40.9	38.0	94.8	85.3
23	4498.0	1743.8	1515.0	40.5	33.7	93.4	87.1
24	4353.0	1744.2	1591.0	41.9	36.5	86.0	69.7
25	4355.0	1777.0	1681.0	42.6	38.6	95.6	91.5
26	4464.0	1777.4	1607.0	41.7	36.0	92.9	80.2
27	4182.0	1724.7	1565.0	42.8	37.4	95.6	86.8
28	1582.0	296.4	216.0	19.8	13.7	57.4	41.3
29	2735.0	1008.6	915.0	38.1	33.5	56.2	54.5
30	517	0.0	-2.0	0.0	0.0	6.2	0.0
31	1928.0	534.2	569.0	30.0	29.5	20.7	16.6
TOTAL	44792.0	16651.7	15187.0	38.8	33.9	65.9	56.2

p: predicted m: measured

Discussion of SVS(1) results in tables 4 and 5 and figures 3 to 6.

In table 4 we have a comparison between measured and calculated efficiencies of the solar collector and measured and calculated solar fraction of heating demand:

$$EFF_p = \frac{QHXI_p}{QSUN} \qquad F_p = \frac{QB - QAUX_p}{QB}$$

$$EFF_m = \frac{QHXI_m}{QSUN} \qquad F_m = \frac{QB - QAUX_m}{QB}$$

(efficiency) (solar fraction)

As expected, the difference between F_p and F_m is greater than for EFF_p and EFF_m because F_p and F_m values represent the final result of how the solar system works.

In table 5 we have a comparison between measured data and the most important SVS(1) results. There is a little difference in the way to measure and calculate the QTO value. The measured QTO is the heat leaving the storage tank, while in the calculation QTO is said to be the heat from the storage tank reaching the building heating system, this is also called QSOP. This means that the right value of QTO calculated would be, QTO = QSOP + QRORTH, so the pipe heat losses would be included. Now QRORTH is only about 1% of QSOP, so it makes very little difference.

In table 5 we have comparisons between the QHXI, QTO and QAUX values and the mean difference $\bar{d}$ and the standard deviation σ_d. The $\bar{d}$ value expresses what the total difference between measured and calculated results is. For instance, if the number of hours is N, then $(QTO_p - QTO_m) = \bar{d} \times N$. And the standard deviation σ_d expresses that we can expect to find 95% of the difference values in the area $\bar{d} \pm \sigma_d$.

There is another statistic value which we also will use, that is the standard error of mean $\sigma_{\bar{d}}$.

$$\sigma_{\bar{d}} = \frac{\sigma_d}{\sqrt{N}} .$$

When you compare measured and calculated values, it is a rule of large sample statistics that if:

$$2 \times \sigma_{\bar{d}} \geq \bar{d}$$

then these values are consistent, and we can consider the hypothesis to be good which says that there is a good agreement between measured and calculated values.

The $\sigma_{\bar{d}}$ values here, for the 14 days period, are:

$\sigma_{\bar{d}}$ (QHXI) = 5.06

$\sigma_{\bar{d}}$ (QTO) = 2.32

$\sigma_{\bar{d}}$ (QAUX) = 3.03

that means that $2 \times \sigma_{\bar{d}} \geq \bar{d}$ will not be true for this period.

Fig. 3 and 4 present a comparison between measured and calculated values, on an hourly basis, of the solar heat from the collectors to the heat exchanger, QHXI. Here you are able to study the differences hour by hour. In fig. 3 and 4 there is an obvious difference in the time the collector begins to produce heat, the reason could be that the effect of heat capacity of the collectors is not taken into account in the collector simulation. This could also be an explanation of the difference in the afternoon.

The comparison of measured and calculated tank temperatures in fig. 5 and 6 shows, together with fig. 3 and 4 and also the tables, that the SVS(1) calculation has calculated too positively, as we had expected it would.

Fig. 3 and 4 show 4 days values of measured and calculated, SVS(1), solar heat from collectors to heat exchanger, QHXI. kWh.

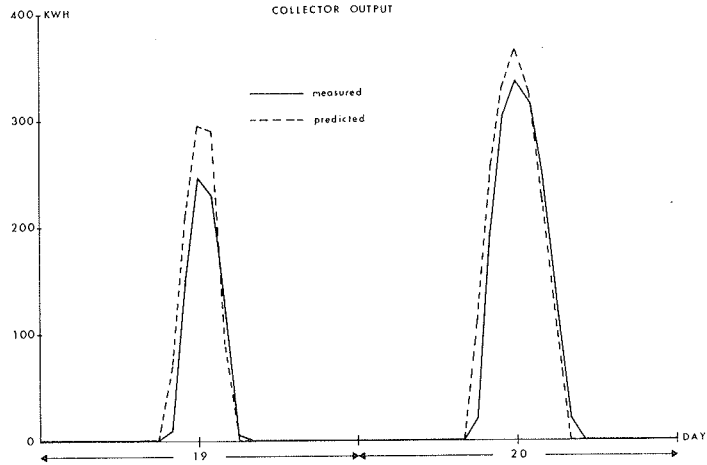

Fig. 3

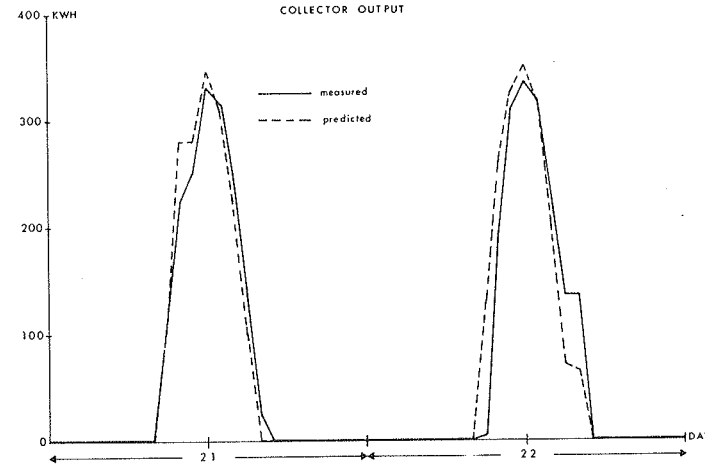

Fig. 4

Fig. 5 and 6 show 4 days values of measured and calculated, SVS(1), storage temperature, ^{o}C

Storage temperature, ^{o}C

Fig. 5

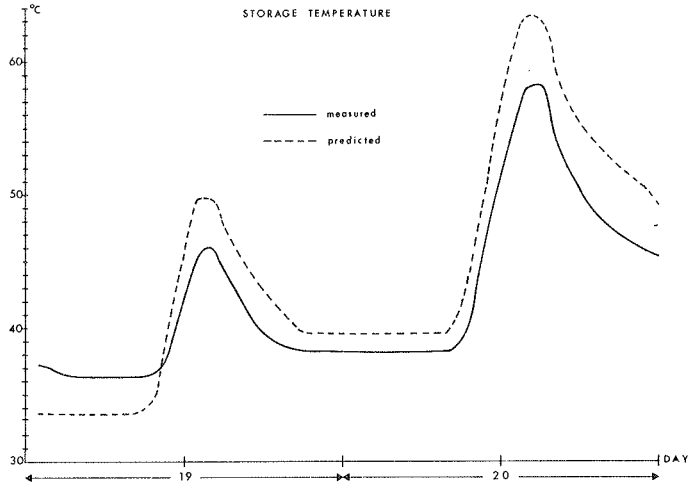

Fig. 6

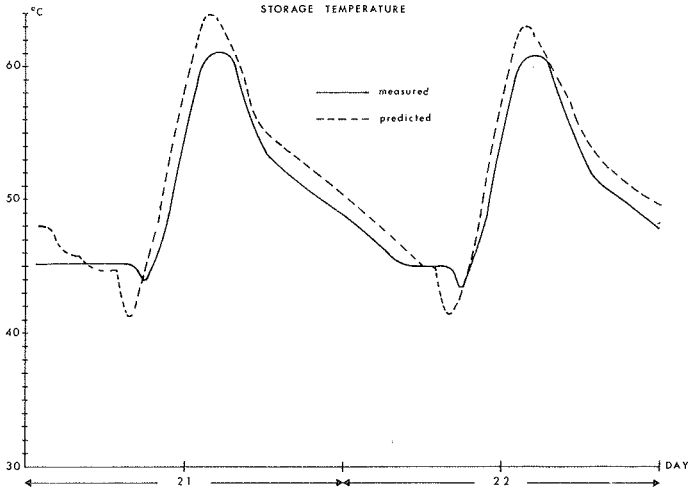

Table 5. ENERGY QUANTITIES, predicted vs. measured (kWh)

DAY	$QHX1_p$	$QHX1_m$	$\bar{d}$	σd	QTO_p	QTO_m	$\bar{d}$	σd	$QAUX_p$	$QAUX_m$	d	σd
18	0	0	-	-	314.0	130.3	23.0	50.4	1391.0	1538.9	-6.2	29.6
19	959.8	775.0	30.8	46.1	675.9	696.6	-1.5	21.4	828.6	834.8	-0.4	22.1
20	1723.1	1566.0	19.6	42.8	1267.2	1173.6	6.2	27.9	648.2	769.2	-11.0	29.4
21	1653.7	1523.0	16.3	50.4	1557.9	1301.6	12.2	37.7	319.4	607.2	-28.8	50.7
22	1708.8	1666,0	5.4	67.4	1716.8	1545.9	7.4	32.4	94.6	322.0	-37.9	54.7
23	1743.8	1515.0	28.6	56.9	1724.3	1608.3	5.0	27.4	121.5	291.2	-42.4	54.8
24	1744.2	1591.0	19.2	53.5	1706.7	1384.3	16.1	38.8	278.1	648.0	-41.1	49.4
25	1777.0	1681.0	12.0	48.9	1743.6	1669.3	3.1	31.9	80.8	209.8	-25.8	68.0
26	1777.4	1607.0	21.3	54.0	1679.1	1448.8	10.0	42.5	127.6	405.0	-34.7	65.2
27	1724.7	1565.0	20.0	55.9	1672.9	1517.9	6.5	39.8	76.8	283.6	-51.7	92.7
28	296.4	216.0	11.5	30.8	887.4	639.5	16.5	34.8	659.8	916.6	-16.0	33.6
29	1008.6	915.0	15.6	51.9	849.5	823.4	1.9	19.2	660.9	706.0	-3.5	23.5
30	0.0	-2.0	-	-	114.5	0.0	-	-	1724.7	1808.0	-3.5	22.9
31	534.2	569.0	-5.8	27.7	371.0	297.4	12.3	56.6	1424.4	1482.5	-2.8	29.6
TOTAL	16651.7	15187.0	16.3	48.0	16280.8	14236.9	8.8	35.3	8436.4	10822.8	-14.0	39.6

CHAPTER III

VALIDATION

Validation of the SVS-program

3.1 Possible reasons for differences

The main reason for the difference between predicted and measured values of the STC-solar system was, as said before, that the SVS collector subroutine calculated too high results. There are several reasons which could be interesting to investigate. We started by looking at the following three:

a) The splitting of Q35 in direct and diffuse insolation.

b) The influence of heat capacity of the solar collector.

c) Examination of the values of collector heat loss, U_L, and the effective transmission, absorption product $(\tau\alpha)_e$ in the collector subroutine.

For the rest of the solar system it might also be interesting to compare heat losses of the storage tank and pipes. And to see which differences are caused by the fact that the SVS-program does not include heat losses in the heat exchanger and in the heat exchanger circuit.

Splitting of the insolation

In the SVS-program we assumed that 75% of the Q35 insolation was direct. To see what influence this could have on the calculations, we also tried to run the program with 65 and 85% direct insolation. We found that the results only changed little, so it seemed right to conclude that the influence of this would not explain the differences between predicted and measured results. We still recommend that direct and diffuse insolation are calculated more accurately than in this SVS-calculation, or even better, that these values could be given as data in later validation work.

The influence of heat capacity of the solar collector

In fig. (1) we have tried, for each hour of the 23/12, to plot the percentual solar gain of the Study Center solar collector as a function of the insolation and the tank temperature. Curve a, b and c are measured values, calculation (1) values, SVS(1), and efficiency curve values from 9 to 15 o'clock.

curve a) plot of $(x, y) = \frac{(TSAV-Ta)}{Q35xSFAK}, \frac{QHXI*1.042}{Q35xSFAK}$

(we assume pipe losses in collector circuit to be 4.2% of QHXI)

- b) plot of $(x, y) = \frac{(TS1-Ta)}{DIN}, \frac{QTIL}{DIN}$

- c) plot of $(x, y) = \frac{(TTANK-Ta)}{I}, \eta r * F'''$

When calculating the actual solar gain of the solar collector, we have to take into account that the tank temperature is not the same as the collector input temperature because of the heat exchanger. We do this by multiplying with F'''.

From fig. 1. you will see that calculation (1) gives about 5% higher efficiencies than the measured data. This agrees quite well with the results from the entire 14 days period.

In chapter 4 we present results from a new collector routine where collector heat capacity is taken into account. One of the goals for this run was to be able to illustrate that collector capacity could have some influence on the results, like the measured data in fig. 1 seem to show. For instance, a lower efficiency in the morning than in the afternoon.

Fig. 1. Percentual solar gain of the collectors as a function of insolation and tank temperature. (For the 23/12 from 9 - 15).

Efficiency of STC-collector, calculated and measured for day 357.

i.e. $\frac{\text{heat from solar collector}}{\text{solar energy to collector}}$

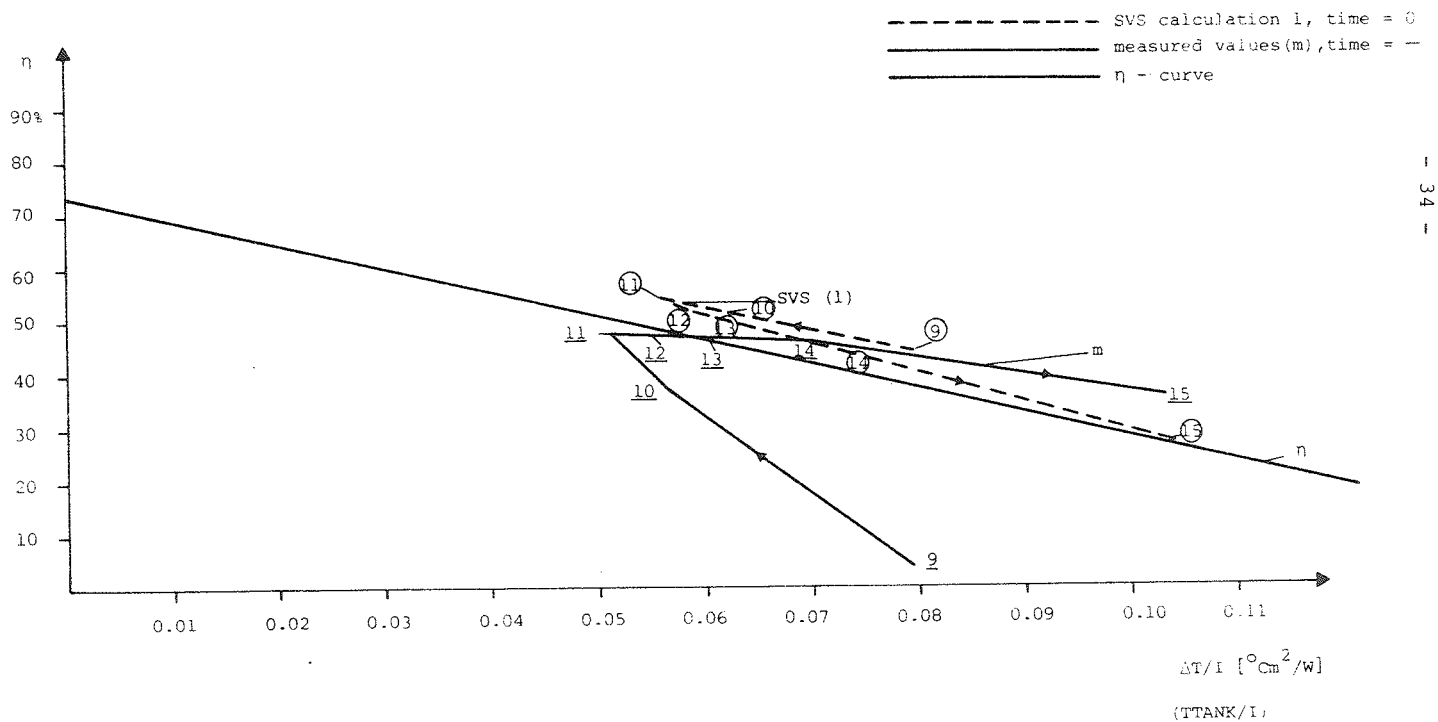

Examination of the values of the collector heat loss coefficient U_L and the transmission absorption product $(\tau\alpha)_e$ in the collector routine.

In fig. 5 we saw that the collector subroutine gives higher gains than the measured efficiency curve would predict. The reason could be the F_R and the F''' values, it could also be too high $(\tau\alpha)_e$ values or too low U_L values. The F' value in the SVS-program is 0.95, and the F'' is calculated to be between 0.971 and 0.975 with a mean of 0.974. That means a mean F_R of F' x F'' = 0.925.

The $(\tau\alpha)_e$ value in the Study Center, SVS-calculation has values between 0.81 and 0.856, with a mean of 0.845. This means a $F_R * (\tau\alpha)_e$ of 0.782, which is 3.5% less than given by measured efficiency curve.

For the 23/12 we have listed the calculated heat loss values of the solar collector in table 1. On that day the U_L-values have a variation between 3.96 and 4.76. It seems to be very much affected by the wind speed, a fact which is also represented by figure 2.

At a characteristic wind speed about 3 m/s, and an ambient temperature about 1 ^oC, the U_L-value will be calculated by the SVS-program to be about 4.2 $W/m^2\ ^oC$.

By using the above-mentioned F_R-value and comparing this to the measured efficiency curve where $F_R \cdot U_L = 4.962$, we find a U_L-value of 5.36 $W/m^2\ ^oC$.

This value is higher than any of those calculated of U_L on the 23/12, and is 21% higher than the mean.

The conclusion must be that the SVS-collector subroutine calculates too low U_L-values for the Study Center collector.

In figure 3 we have tried to plot the actual STC-collector efficiency curve (m) x F''' as a function of (TTANK-Ta)/I, and for comparison the SVS-calculated (1) curve. For low values of (TTANK-Ta)/I the calculated efficiency is less than the measured, and for values greater than 0.02 the

opposite is true. The reason is that $(\tau\alpha)_e$-value is also calculated a little bit too low (2.5%). At a typical combination of TTANK = 50 °C, Ta = 0 °C and I = 800, (TTANK-Ta)/I = 0.063, the SVS-calculation will be 5% too positive.

The Study Center solar collector is selective, that means that the radiative heat losses between absorber and glass become much smaller than the convective losses. Because of this it would be reasonable at a first step to see if it is possible to improve the calculation of the convective heat loss between absorber and the glass. And the next step must then be to look at the heat loss from glass to the ambience. For this report we have only had time to investigate the first step.

Fig. 2.

U_L as a function of windspeed.

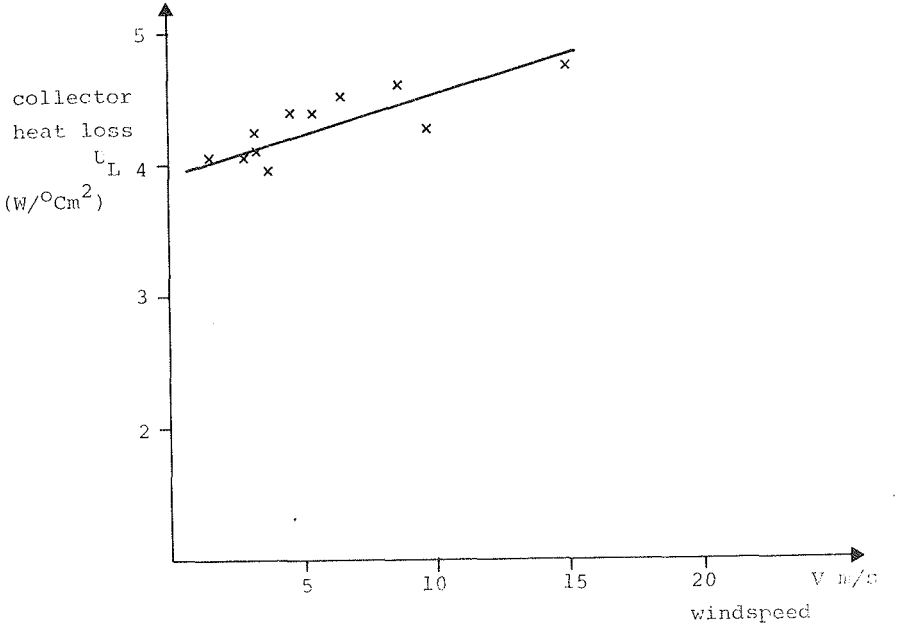

Table 1. Collector heat loss values, U_L, for the 23/12, 78.
Calculation (1), Study Center, SVS(1)

DAY	hour	V(m/s)	Ta(^{o}C)	$h_{r,1}$	$h_{c,1}$	$h_{r,2}$	$h_{c,2}$	U_L (W/m^2 ^{o}C)
		windspeed	ambient temperature	absorber glass radiation	absorber glass convection	(glass, ambient) radiation	convection	collector heat loss
23	8	3.8	-1.1	0.49	3.11	3.81	13.1	3.96
-	9	2.8	0.7	0.55	3.36	3.98	11.1	4.06
-	10	3.2	2.1	0.56	3.42	4.05	11.9	4.12
-	11	1.5	1.9	0.59	3.48	4.12	8.60	4.04
-	12	5.5	0.8	0.60	3.63	4.02	16.4	4.39
-	13	6.5	0.7	0.61	3.70	4.02	18.4	4.49
-	14	4.7	1.2	0.62	3.70	4.08	14.8	4.41
-	15	14.9	-1.1	0.60	3.76	3.91	34.8	4.76
-	16	3.1	-0.4	0.60	3.62	4.01	11.7	4.24
20	8	9.9						4.23
-	14	8.6						4.60

*) U_L is based on the tank temperature as input temperature

Fig. 3. Comparison between the efficiency of the Study Center solar collector, measured and calculated, SVS(1).

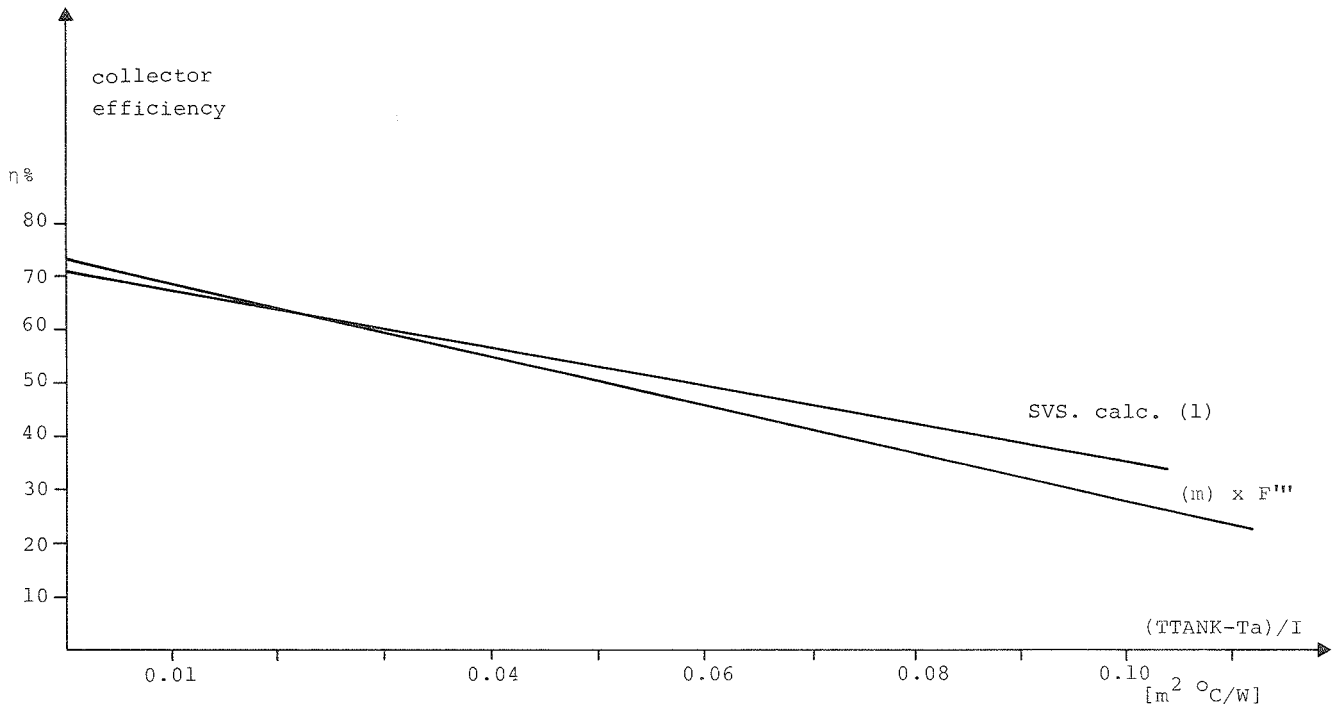

(m) = measured curve.

3.2 Improvement of the collector calculation

Introduction of collector heat capacity to the SVS-program.

The calculation of heat capacity, which we have tried to add to the SVS-program in the subroutine STYR, is illustrated in the flow chart in figure 4. The new parameters introduced here are:

TCT	= TS1 + 5.4°C, pump control temperature	(°C)
TSF	modified plate temperature	(°C)
TSFG	mod. plate temp. the hour before	(°C)
HCS	= 5.667 Wh/m^2 °C, collector heat capacity	
SOKA	heat stored in the collector *)	(J)
QA2R	reduced, absorbed solar heat	(J)

There are four different possibilities of running through the flow chart in figure 1.

a) Pump is off, QA2R is less than 0. TSF is calculated and used for the next hour as TSFG. In the morning f.ex. the collector has to be heated up before QA2R becomes bigger than 0.

b) Pump is off, now QA2R > 0. If the collector is heated to a temperature more than TS1 + 5.4°C, FLOW is calculated, pump is on, and the collector routine is called again, now with FLOW > 0.

c) Pump is on. QA2R will be higher than zero as long as QA2 has a reasonable size because (TC1 - TSFG) is little. TSF and QSOL are calculated.

d) Pump is on. QA2R < 0. TSF is calculated, and pump goes off.

*) When the collector plate temperature is higher than the hour before, some of the absorbed solar heat will be used to heat the collector up to the new temperature.

- In hour no. one TSF and TSFG are assumed to be the same as the ambient temperature.

Fig. 4. Flowchart for the collector heat capacity calculation in STYR

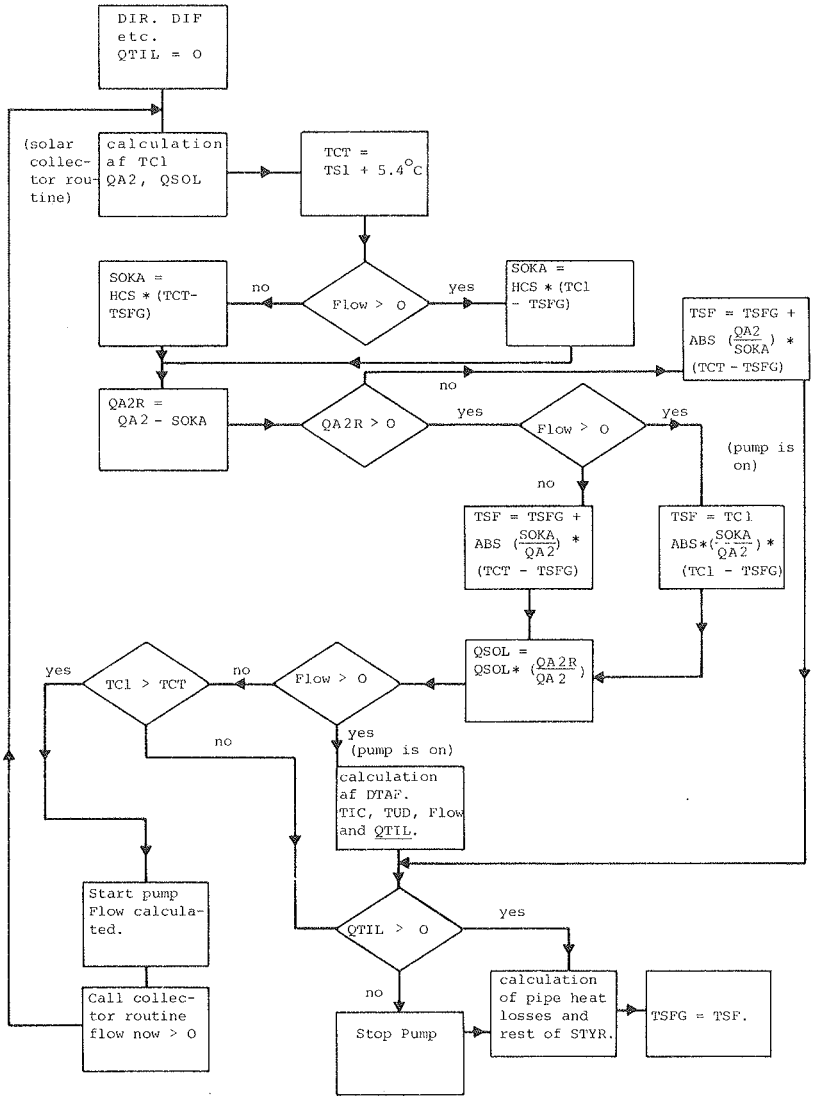

Calculation of convection heat loss between absorber and glass in the solar collector.

This is calculated in the SVS-program as [3]:

$$h_{c,1} = (0.24 - TILT \cdot 10^{-3}) \cdot 5.68 \cdot \frac{9}{5} \cdot (T_1 - T_2)^{0.25}$$

$h_{c,1}$ is here only a function of the tilt and the plate and the glass temperatures. But in fig. 5 [8], it is seen that the separation L between the plate and the glass is also an important factor.

Fig. 5

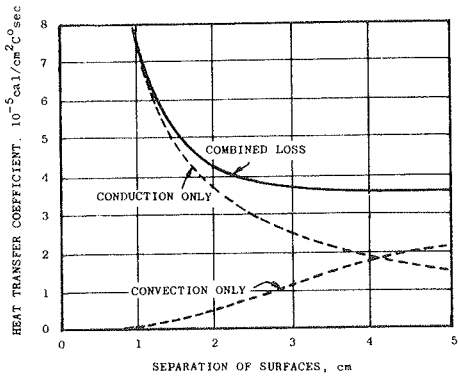

Fig. 10.13 Relationship between heat-transfer coefficient h and the separation of two horizontal surfaces L, for the case where Ra = 8000 for L = 5.0 cm.

We have tried to use a new equation for convection heat loss which is recommended by K.G.T. Hollands et al in Journal of Heat Transfer [6], here the separation is also a parameter.

Hollands et al:

$$h_{c,1} = \frac{N_u \cdot k}{L} \quad ,$$

$$Nu = 1 + 1.44 \cdot \left(1 - \frac{1708}{Ra \cdot \cos\phi}\right) \cdot \left(1 - \frac{(\sin 1.8\phi)^{1.6} \cdot 1708}{Ra \cdot \cos\phi}\right) + \left(\frac{Ra \cos\phi}{5830}\right)^{1/3} - 1 \quad , \quad \phi = \text{TILT} = 60^{\circ}$$

$$Ra = \frac{g \cdot (T_1 - T_2) \cdot L^3}{\nu \cdot \alpha \cdot T_m} \quad , \quad \alpha = \frac{k}{c_p \cdot L}$$

Nu:	Nusselt's number	
k:	Thermal conductivity of air	($W/m^{\circ}C$)
L:	separation, with air layer	(m)
Ra:	Rayleigh's number	
g:	acceleration of gravity	(m/s^2)
ν:	kinematic viscosity	(m^2/s)
T_m:	mean temperature = $(T_1-T_2)/2$	($^{\circ}C$)
$h_{c,1}$:	convective heat loss	($W/m^{2\circ}C$)

For air: $\nu = (13.5 + 0.092 \cdot (T_1 - T_2))$

$\alpha = (19 + 0.134 \cdot (T_1 - T_2))$

$k = (24.4 + 0.072 \cdot (T_1 - T_2))$

3.3 SVS-simulation (3) using improved collector subroutine

As expected these changes resulted in less solar gain from the collector. The results are presented in tables and curves in the next chapter, but the main conclusion is that there is now a much better agreement between measured and calculated values. Table 2 presents the results of the whole period.

Table 2.

	Measured data	SVS(1)	SVS(2) (with collector capacity)	SVS(3) (with collector capacity and new convection calculation)
QCOLL	15817	17337	16069	16012
QHXI	15187	16652	15435	15382
QTI	14901	16652	15435	15382
QTO	14237	16316	15086	14989
QSOP	14207	16281	15051	14954
QAUX	10823	8436	9667	9764

The results marked with _____ are extrapolated by using the following mean values, calculated in the SVS-program.
QRORT = 630 kWh, pipe heat loss in collector circuit.
QRORTH = 35 kWh, pipe heat loss in heating circuit.

The difference between calculated and measured QHXI values are from calculation 1 to 3 reduced from 1465 kWh to 195 kWh, mainly because of the introduction of collector capacity.

Improvement of convection calculation

To investigate how the new convection calculation has worked compared to the old one, the QHXI results of different L values are presented in fig. 6. The L value for the STC-collector has been reported from Jim Hedstrom to be 1 inch, which is about 2.5 cm. In this case the new convection calculation only meant a reduction in the QHXI value of 53 kWh. (15435 to 15382 kWh).

Fig. 6. Solar fraction versus glass-absorber space.

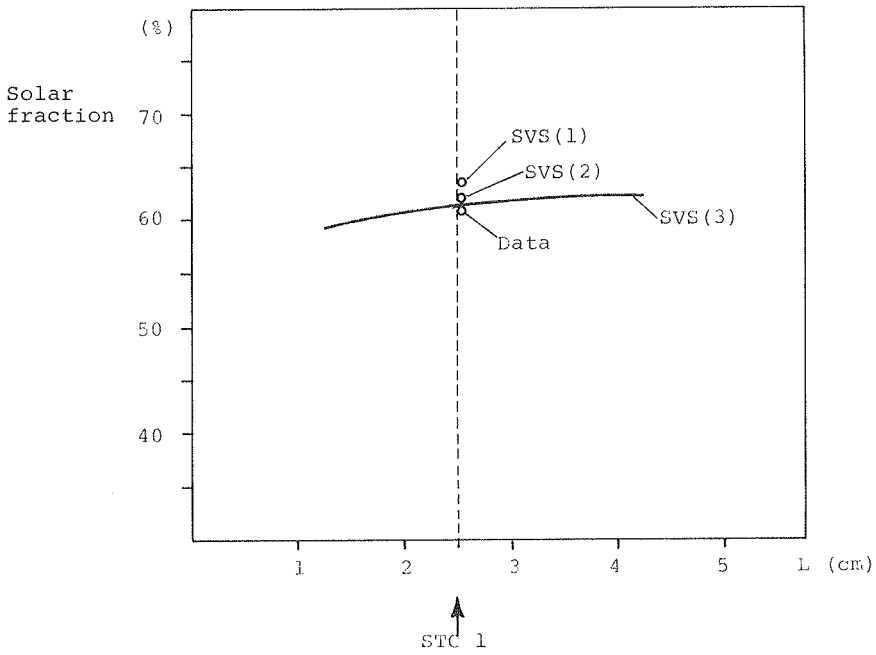

Space between absorber plate and the glass in the collector.

3.4 Influence of heat capacity on solar collector performance

In tables 3 and 4 we have listed the hourly results of the two calculations and compared with measured values and a new calculation SVS(4) which is based upon the measured efficiency curve instead of the collector routine, but still with collector capacity. The comparison is for day 357 = 23/12-78. The results are plotted in figures 7, 8 and 9.

In fig. 8 (which is made in the same way as fig. 1 in this chapter) it is seen that the new way of calculating the solar collector gives results which are better compared to the measured, and where the collector seems to work in the same way as the measured data are showing. That means that the efficiency is growing up in the first hours near to the efficiency curve, and growing higher than the curve in the afternoon. It works better in the morning than in the afternoon compared to the measured curve (m). The influence of collector heat capacity is still not as high in the SVS results as curve (m) seems to show. Around noon the collector capacity should only have very little influence. Here fig. 8 still shows a little higher efficiency values of the calculated data than the measured. The U_L values of day 357 have values between 4.07 - 4.78 $W/m^2\ ^oC$, which are lower than the measured efficiency curve would predict. The influence of this can be seen in fig. 9, where SVS(4) is also plotted.

Day no. 357 = 23/12, 78, is a day with good sunshine. We have marked the two actual running areas A and B in fig. 10, where also the comparison of the measured efficiency curve η_m and the SVS-calculated $\eta_{SVS(3)}$ can be seen.

Table 3. In table 3 and 4 we have hourly results for day 357 of SVS(1), SVS(3) and SVS(4) compared to the measured data.

		SVS-calculation 1.								measured data. (**)					
	hour	DIN kw	I_2 W/m^2	QTIL kw	$\frac{QTIL}{DIN} = \eta_1$	T_a (^oC)	TS1 (^oC)	ΔT (^oC)	$XPM_c = \frac{\Delta T}{I}$	Q35 x SFAK KW	QH x I KW	η_m (*)	TSAV (^oC)	ΔT	$\Delta T/I$
1	9	373.6	522	160.8	0.43	0.7	42.3	41.6	0.080	370.2	11	0.031	42.1	41.3	0.079
2	10	541.4	746	281	0.52	2.1	46.6	44.5	0.060	537.5	194	0.376	44.3	42.2	0.0565
3	11	644.7	901	346.9	0.54	1.9	52.1	50.2	0.056	641.2	289	0.47	48.1	46.2	0.0513
4	12	698.0	975	357.2	0.51	0.8	57.5	56.7	0.058	698	318	0.475	52.3	51.5	0.0528
5	13	680.5	951	325.9	0.48	0.7	61.8	61.1	0.064	680	303	0.464	55.9	55.2	0.058
6	14	581.5	812	245.2	0.42	1.2	64.1	62.9	0.077	573	251	0.456	58.3	57.1	0.070
7	15	406.0	567	90.0	0.22	-0.1	62.9	63.0	0.111	388	133	0.36	58.2	58.3	0.103

$QTIL = F''' \times F_R \times (I \cdot (\tilde{\tau}\alpha)_e - U_L (TS1 - T_a))$ SVS, calculated

$QTIL = F''' \times (0.81 \times I - 4.962 \times (TS1 - T_a))$ η_m, calculated

$* \eta_m = \frac{1.042 * QHXI}{Q35 * SFAK}$, (4,2% pipeloss)

Table 4.

Day 357.

		SVS - calculation 3						SVS - calculation 4, (with measuret officienly and collector capacity).						η -curve	
		QTIL kw	$\frac{QTIL}{DIN}$ = η_3	TS 1 (°C)	(TS 1 - Ta) (°C)	$XPM_{c,3}$ = $\Delta T/I$		QTIL kw	$\frac{QTIL}{DIN}$ = η_4	TS 1 (°C)	(TS 1- Ta) (°C)	$XPM_{c,4}$ = $\Delta T/I$		$\frac{\Delta T}{I}$	$\eta_r \times F'''$
1	1	94.4	0.252	40.6	39.9	0.076		89	0.238	42	41.3	0.079		0.02	0.647
2	10	243	0.449	44	41,9	0,056		241	0.445	44	41,9	0.0554		0.04	0.556
3	11	332.3	0.515	49,2	47,3	0.0525		326	0.505	46,8	64,8	0.052		0,06	0.466
4	12	352	0.504	54.5	53.7	0.055		349	0.50	53,6	52.8	0,0542		0.08	0.376
5	13	324,3	0.477	58.9	58.2	0.061		322	0.473	57.6	56.9	0,060		0.10	0.286
6	14	249.2	0,429	61,4	60.2	0.074		242	0.416	59.4	58.3	0.072			
7	16	101.7	0.25	60.9	61.0	0.107		106	0.261	58.8	58.9	0.104			

Fig. 7.

Solar energy to the collectors, DIN, and collector output to the heat exchanger, QHXI, measured and calculated for day 357.

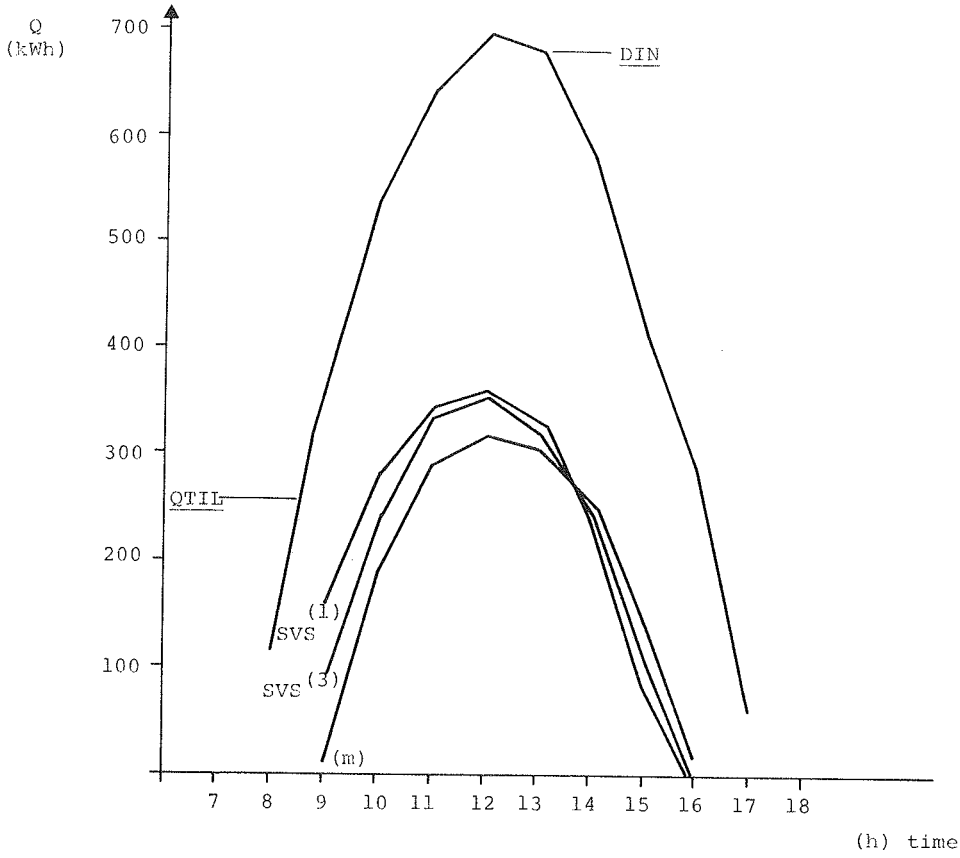

Fig. 8.
Efficiency of STC-collector, calculated and measured for day 357 from 9 to 15.

$$\eta_c = \frac{\text{heat from solar collector}}{\text{solar energy to collector}}$$

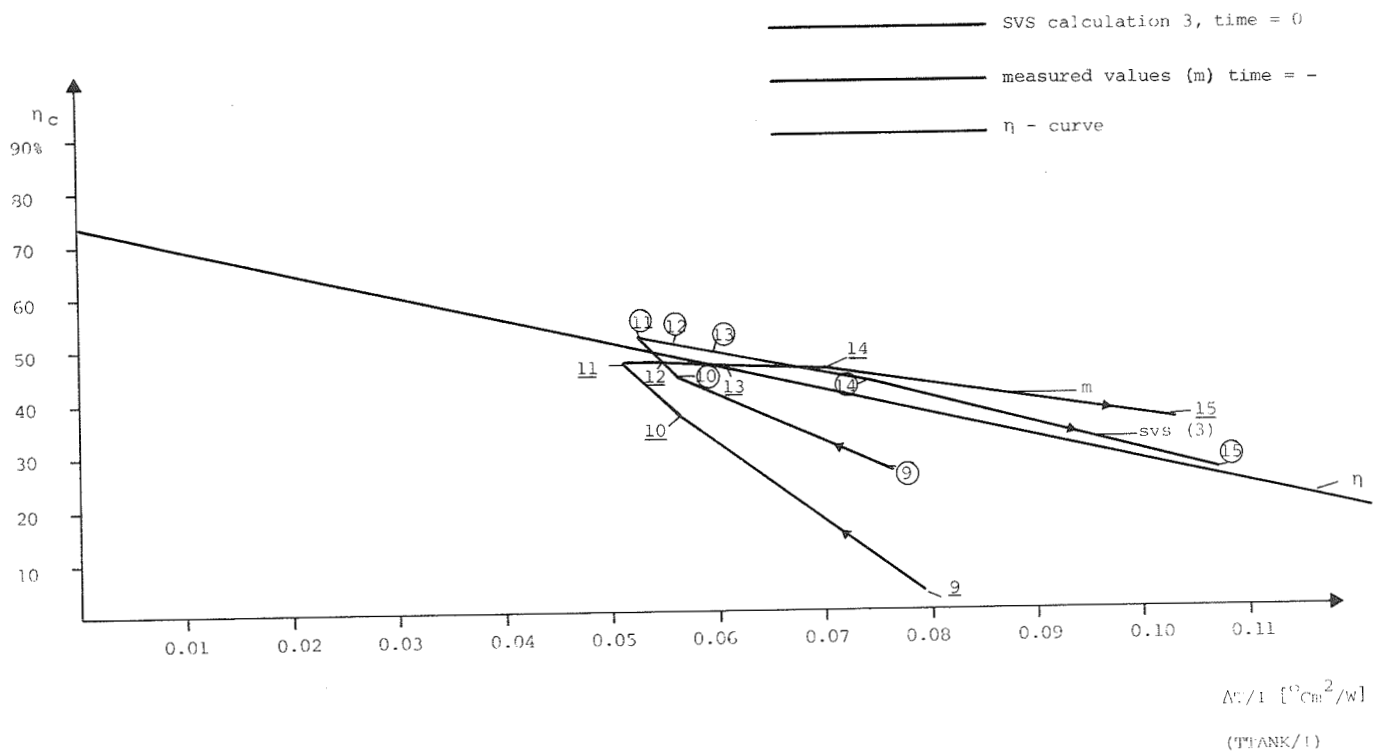

Fig. 9.

Efficiency of STC-collector, calculated and measured for day 357. from 9 to 15.

η_c = heat from solar collector / solar energy to collector

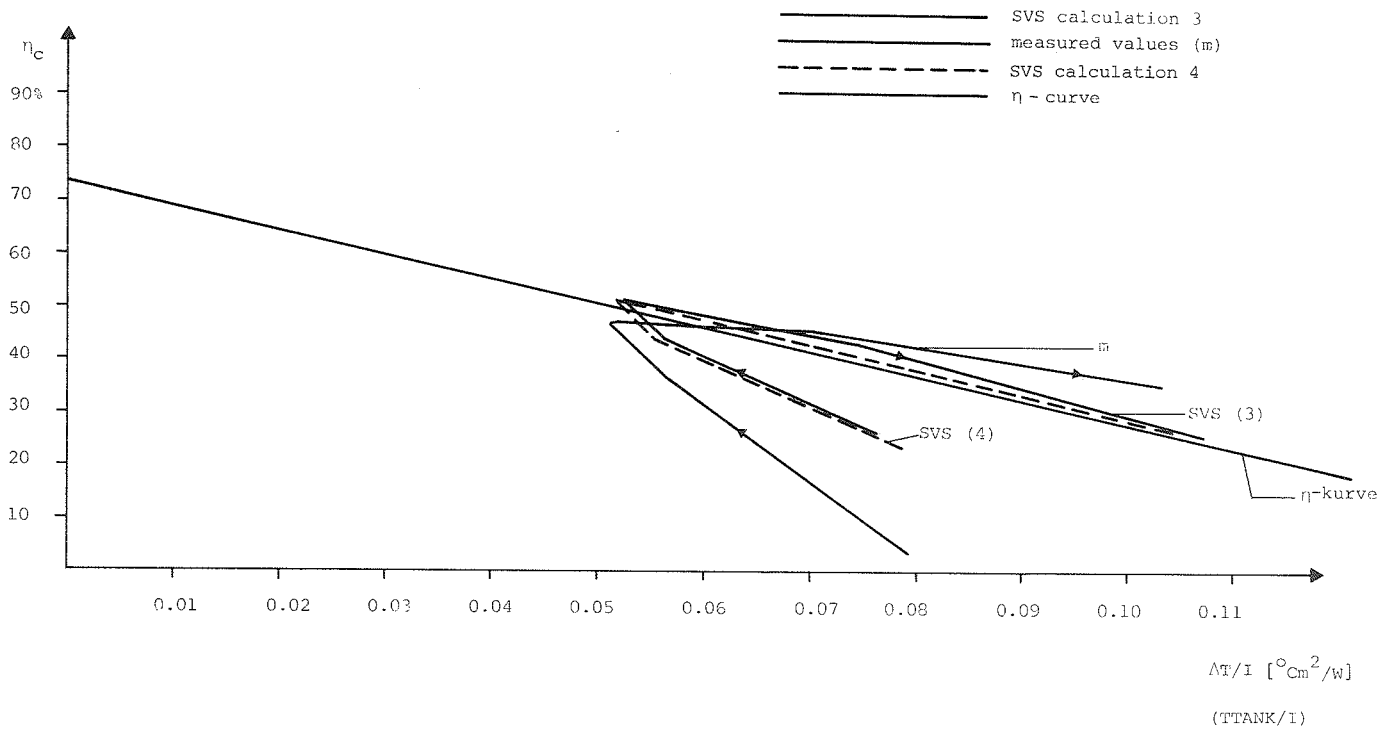

Fig. 10. Comparison between the efficiency of the Study Center solar collector measured and calculated, SVS(3).

STC - SOLAR COLLECTOR

day 357 A h. 11-13 diff.: +3.8%

B h. 9,-10, 14-15. diff. +(3.3-3.9%)

XPAR	η_R(%)	η_m(%)
0	79.7	81
0.01	76.3	76.0
0.02	72.4	71.1
0.03	68.3	66.1
0.04	64.0	61.2
0.05	59.5	56.2
0.06	54.8	51.2
0.07	50.1	46.3
0.08	45.2	41.3
0.09	40.2	36.3
0.10	35.0	31.4

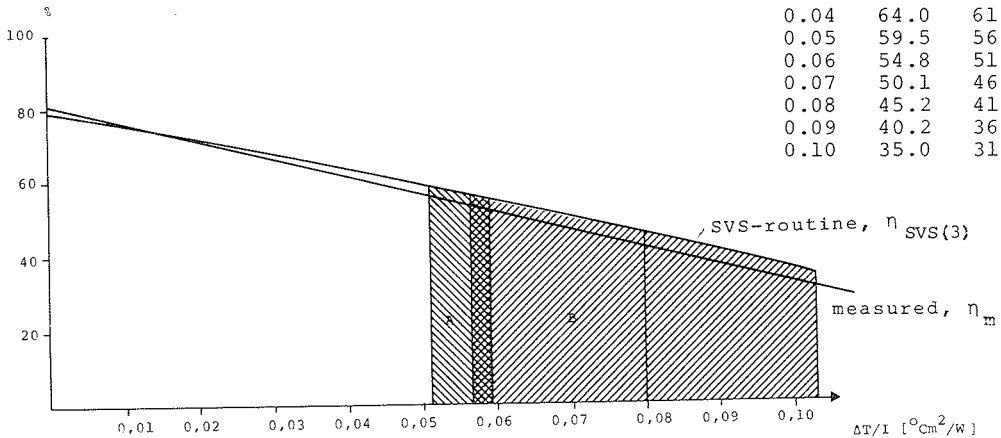

VHA = 3 m/s, Ts = Ta = 0 °C, FLOW = 2.5 L/s, m^2_c

VIN = 0, DIR = 1000 $\frac{W}{m^2}$, DIF = 0 $\frac{W}{m^2}$, TIND = 0 °C - 100 °C

$$XPAR = \frac{(TIND - Ta)}{(DIR + DIF)} = 0,\ 0.01,\ 0.02\ \text{----}\ 0.10.$$

CHAPTER IV

THE FINAL COMPARISONS

4.1 Final SVS-version compared to measured data

The comparisons are presented in this paragraph in accordance with ref. [7].

Table 2 shows that there is a very good agreement between measured and calculated efficiencies EFF_p and EFF_m, while there is still some difference, but much smaller, between solar fractions F_p and F_m. That is because there is still a difference between heat loss calculations and measured values here.

Table 3 shows a good agreement between measured and calculated results, also for the different days.

In table 4 and 1 we see that the $\bar{d}$ values have changed from the SVS(1) calculation, while the σ_d and $\sigma_{\bar{d}}$ only have changed little.

Table 1. Difference, standard deviation and standard error of mean, for the SVS(1) and SVS(3) calculations.

		$\bar{d}$	σ_d	$\sigma_{\bar{d}}$
QHXI	SVS(1)	16.3	48.0	5.06
	SVS(3)	2.17	29.2	3.07
QTO	SVS(1)	8.8	35.3	2.35
	SVS(3)	3.2	31.9	2.14
QAUX	SVS(1)	-14.0	39.6	3.03
	SVS(3)	-6.2	35.8	2.73

Table 1 gives a very good picture of the difference between the SVS(1) and SVS(3) calculations. The SVS(3), $\bar{d}$ value for QHXI is now very small because the collector simulation gives results which are near to the measured data. And the $\bar{d}$ value of QAUX is still quite big. This also means that $2 \times \sigma_{\bar{d}} > \bar{d}$ is true for QHXI, but for QAUX $2 \times \sigma_{\bar{d}}$ is a little bit higher than $\bar{d}$. This shows that if we made a run with a little bit better simulation of system heat losses than in the SVS(3) calculation, then it should be possible also to have $2 \times \sigma_{\bar{d}} > \bar{d}$ for QAUX.

In fig. 1 and 2, where we have the hourly values of collector output, QHXI, we see that there is a much better agreement between measured and calculated values in the SVS(3) calculation than in the SVS(1) calculation. If you compare fig. 3 and 4 in chapter 2, you will see that the difference in the morning and in the afternoon has really changed. In fig. 3 and 4 with the tank temperature you can see that the difference has become smaller, especially for the days with good sunshine, 21 and 22.

The conclusion must be that we now have shown that the SVS(3) simulation model can give results in good agreement with measured values.

Presentation of the SVS(3) run on the Study Center solar heating system with December 78 data.

PERFORMANCE VALUES

predicted vs. measured

Table 2

	⌜ collector output ⌝						
DAY	QSUN (kWh)	$QHXI_p$ (kWh)	$QHXI_m$ (kWh)	EFF_p (%)	EFF_m (%)	F_p (%)	F_m (%)
18	654.0	0.0	0.0	0.0	0.0	18.4	7.6
19	2320.0	884.4	775.0	38.1	33.4	42.3	46.3
20	4500.0	1589.9	1566.0	35.3	34.8	60.5	61.3
21	4323.0	1535.8	1523.0	35.5	35.2	80.4	69.3
22	4381.0	1595.9	1666.0	36.4	38.0	87.3	85.3
23	4498.0	1641.9	1515.0	36.5	33.7	90.2	87.1
24	4353.0	1560.3	1591.0	35.8	36.5	74.5	69.7
25	4355.0	1660.7	1681.0	38.1	38.6	90.9	91.5
26	4464.0	1640.5	1607.0	36.7	36.0	83.6	80.2
27	4182.0	1589.6	1565.0	38.0	37.4	89.3	86.8
28	1582.0	235.7	216.0	14.9	13.7	46.5	41.3
29	2735.0	947.6	915.0	34.6	33.5	53.8	54.5
30	517	0.0	-2.0	0.0	0.0	6.1	0.0
31	1928.0	500.2	569.0	25.9	29.5	13.5	16.6
TOTAL	44792.0	15382.5	15187.0	34.3	33.9	60.5	56.2

p: predicted m: measured

Table 3

ENERGY QUANTITIES, predicted vs. measured (kWh)

DAY	$QHXI_p$	$QHXl_m$	$\bar{d}$	σd	QTO_p	QTO_m	$\bar{d}$	σd	$QAUX_p$	$QAUX_m$	$\bar{d}$	σd
18	0	0	-	-	314.0	130.3	23.0	50.4	1391.0	1538.9	-6.2	29.6
19	884.4	775.0	18.2	34.7	636.4	696.6	-4.6	18.6	868.1	834.8	2.1	19.0
20	1589.9	1566.0	3.0	23.5	1159.1	1173.6	-1.0	8.4	756.3	769.2	-1.2	13.3
21	1535.8	1523.0	1.6	28.0	1508.9	1301.6	10.4	37.7	368.4	607.2	-23.9	50.8
22	1595.9	1666.0	-8.8	44.0	1582.2	1545.9	1.6	36.9	229.2	322.0	-15.5	74.4
23	1641.9	1515.0	15.8	34.2	1664.2	1608.3	2.4	25.4	181.6	291.2	-27.4	54.7
24	1560.3	1591.0	-3.8	22.6	1472.3	1384.3	5.2	23.5	512.5	648.0	-15.1	35.2
25	1660.7	1681.0	-2.5	27.7	1657.6	1669.3	-0.5	24.8	166.8	209.8	-8.6	58.6
26	1640.5	1607.0	4.2	30.6	1510.0	1448.8	2.9	35.8	296.7	405.0	-13.5	56.7
27	1589.6	1565.0	3.1	30.7	1563.2	1517.9	2.0	34.0	186.5	283.6	-24.3	87.2
28	235.7	216.0	2.8	20.8	719.7	639.5	5.3	48.6	827.5	916.6	-5.2	44.6
29	947.6	915.0	5.4	35.0	812.0	823.4	-0.9	16.8	698.4	706.0	-0.6	20.7
30	0	-2.0	2.0	0	112.4	0.0	112.4	0	1726.8	1808.0	-3.4	22.7
31	500.2	569.0	-11.5	19.7	241.6	297.4	-9.3	19.4	1553.8	1482.5	3.4	11.9
TOTAL	15382.5	15187.0	2.17	29.2	14953.6	14236.9	3.2	31.9	9763.6	10822.8	-6.2	35.8

4 days measured and calculated values, SVS(3)
of solar heat from collectors to heat exchanger, QHXI

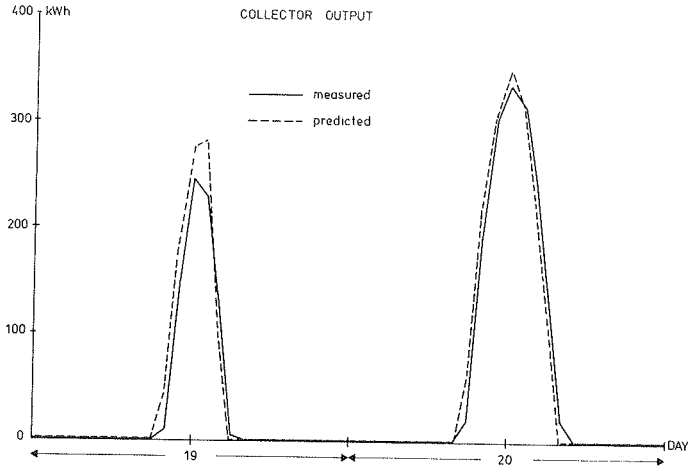

Fig. 1

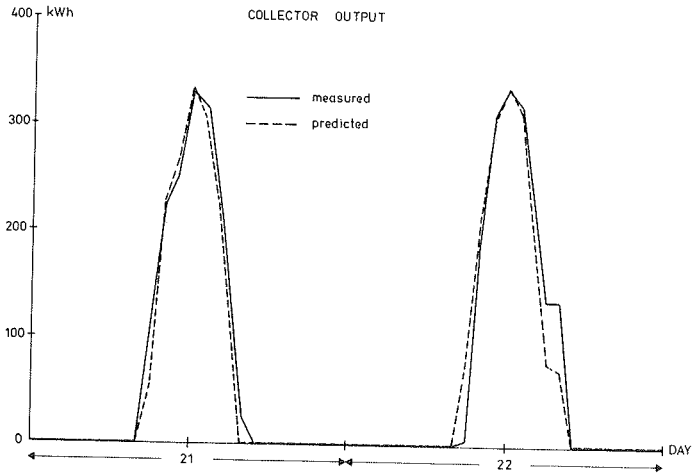

Fig. 2

4 days measured and calculated values, SVS(3)
of the storage temperature.

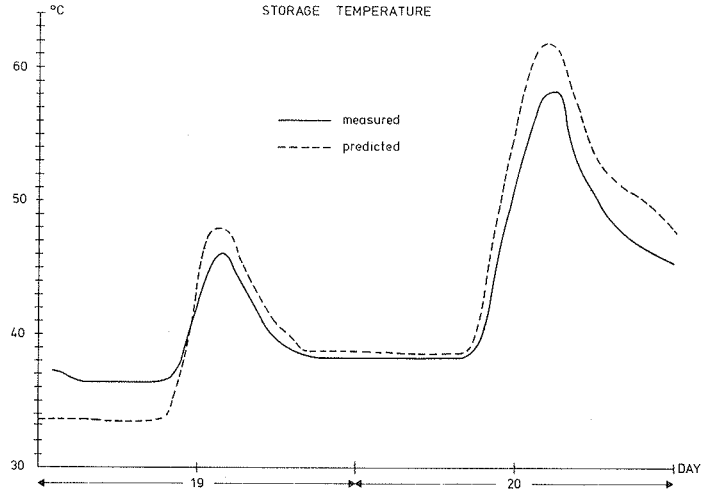

Fig. 3

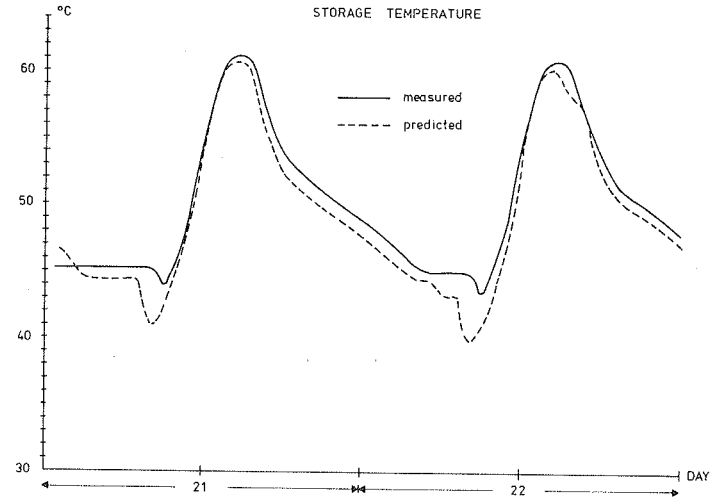

Fig. 4

4.2 Possible reasons for differences

From fig. 5 and table 5 it is seen that there has been a substantial improvement of the collector calculation, and that this means better agreement between measured data and the SVS-results.

The SVS(3) calculation reduces the difference between calculated and measured results to 195 kWh when we consider the QHXI value. The QSOP difference, which in the first calculation was 2387 kWh is reduced to 1060 kWh.

The difference between the 1060 kWh and the 195 kWh = 865 kWh is explained in fig. 5 and table 5.

There are three reasons:

1. The SVS-program does not calculate heat losses in heat exchanger and heat exchanger circuit (286 kWh).
2. There is a difference between measured and calculated storage tank losses (271 kWh).
3. There is a difference between measured and calculated heating pipe heat losses (308 kWh).

The sum of 1., 2. and 3. is 865 kWh. Most of the difference in 2. and 3. is because the measured heat losses have been greater than theory would predict. This is due to 494 kWh.

As a conclusion on the matter of the solar system heat losses, it must be said that the pipe heat losses of the collector circuit seem to be calculated about 50% too low compared to ideal. As to the heat losses from the heat exchanger and heat exchanger circuit, it must be recommended to include these. And for the heat losses from storage and heating pipes, there seems to be quite good agreement between the calculated and the ideal results, but there will often be higher measured losses than ideal.

Fig. 5. Comparison between measured (m) and calculated, SVS(1) and SVS(3) values. For the December 78, 14 days period. Energy flow and heat losses in the system.

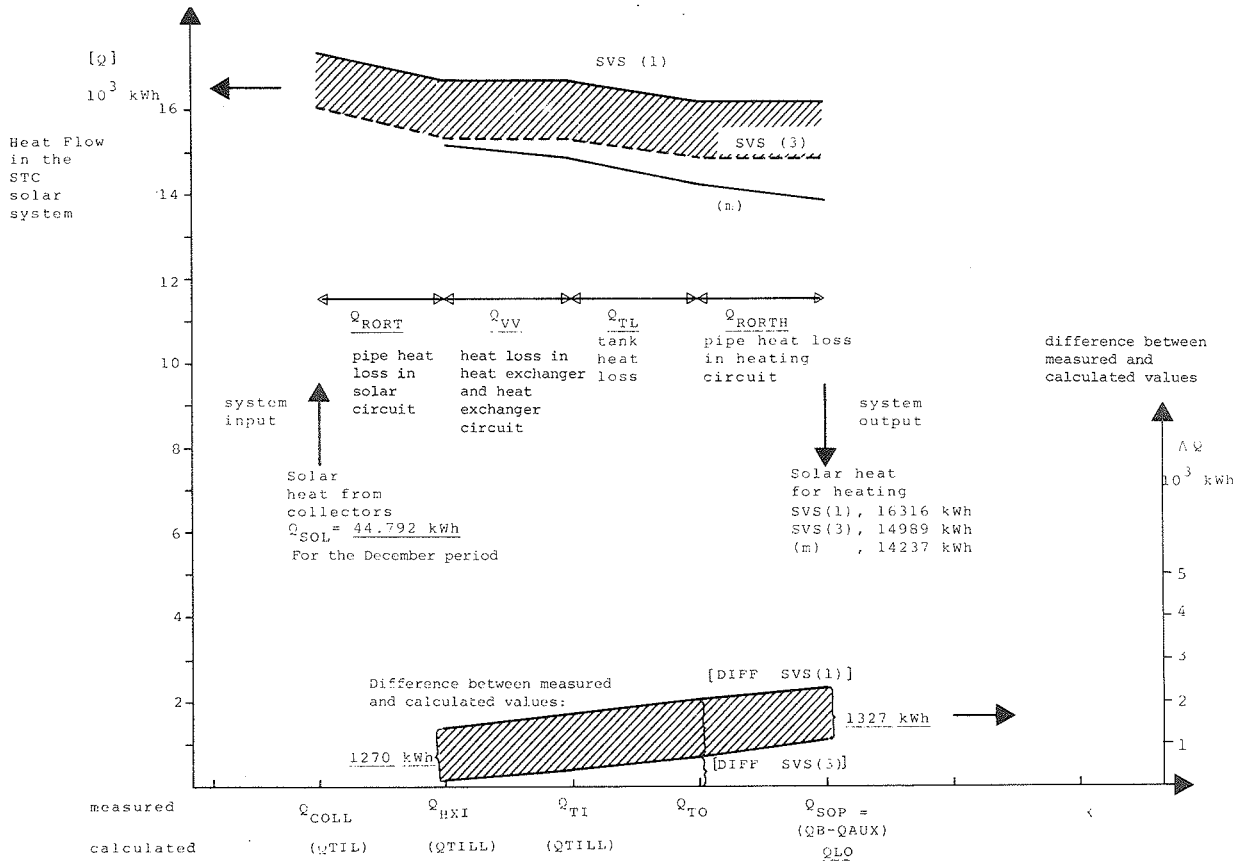

Table 5. Results of Study Center calculated by Dec. 78 data (18/12 - 31/12) QSUN = 44.792 kWh
QB = 24.717 kWh

	Q_{coll}	QHXI	QTI	QTO	QSOP	QAUX	TSAV	% sol
measured, (m)	15817	15187	14901	14237	(QB-QAUX) = 13894	10823	44.9	56.2
SVS(1)	17337	16652	16652	16316	16281	8436	45.6	65.9
SVS(3)	16012	15382	15382	14989	14954	9764	44.5	60
difference (D1) (SVS(1) - (m))		1465	1751	2079	2387	2387		
difference (D2) (SVS(3) - (m))		195	481	752	1060	1060		
(m), decrease from previous		(Q_{coll} → QHXI) 630 (theory)	(QHXI → QTI) 286	(QTI → QTO) 664	(QTO → QSOP) 343			
SVS(3) decrease from previous		630	0	394	35			
D2 - increase from previous		195	286	271	308	0		
reason for D2 - increase		collector routine still too positive	heat loss of heat exchanger not calculated	QTL measured higher than theory	QRORTH too little			

(___) means extrapolated values.

Table 6.

Discussion of heat losses (HL), calculated and measured.

	HL in SVS (3) A (kWh)	HL-coefficient from data. B (W/°C	hours in the 336 h period	ΔT (°C)= A/B	this means a mean temperature (°C)	HL measured (kWh)	This means a mean temperature (°C)	Expected mean temperatures (°C)	HL predicted if ideal (kWh)
1. pipe heat loss in collector for circuit	630	285	95	23.2	44.3	630	44.3	55	921
2. heatloss in heat exchanger and h.e. circuit	0	70.9	95	0	21.1	286	63.6	50	196
3. pipe heatloss in heating circuit	35	35.3	196	5	26.1	383	76.4	45	165
4. storage tank heat loss.	394	45.8	336	25.6	46.7	664	64.7	45	390

Discussion of heat losses from pipes and storage, measured and calculated

Table 6 shows that the tank heat loss seems to work all right, while the other heat losses are too small. It also shows that the measured heat losses have higher values than the ideal, except for the collector circuit loss. The difference between the total heat losses in the SVS (3) system and what is measured is 864 kWh. The difference between SVS (3) and the ideal could be calculated as, 613 kWh.

This indicates that the measured heat losses are 251 kWh higher than theory would predict, and if we only consider the no. 2, 3 and 4 heat losses, the measured heat losses are 582 kWh higher than the ideal.

CHAPTER V

CONCLUSIONS

Conclusion

The conclusion of the Study Center validation work is that if the SVS-program is used to simulate a well described solar heating system of this type, the calculation results agree reasonably well with the measured results.

It is important to emphasize that an accurate simulation implies correct information about the solar heating system. That is to say storage losses, tube losses, measured efficiency of solar collectors, efficiency of heat exchangers, control of solar collector pump and of the heating system. Furthermore, certainty of the solar heating system working as wanted during the calculation period, for instance without natural circulation.

In the original SVS-version the too high solar collector efficiency and too high system losses counterbalanced each other, and therefore the calculation results agreed well with the measured results. Within the validation work on the Study Center solar heating system data we have altered the SVS-program so that calculations on the solar collector and the solar heating system agree better with the reality. However, in this connection we shall draw the attention to the fact that especially solar collector calculations still need some analysis work, which, for example, can be done in the validation work to come.

Now, a further validation of the SVS-program must aim at running the program on other types of solar heating systems in other sorts of climates. This might result in other alterations than those suggested by us and should contribute to a more detailed account of the different heat flows in the systems and with this a greater accuracy of the SVS-program. The final aim of the validation work must be to get to a position where it is possible, by means of the SVS-program, to get reliable predictions for many different solar heating systems.

In the further validation work it is recommendable to run two different periods, which means that the first period can be used as an initial experiment where an analysis of differences between measured and calculated results can be utilized for alterations and adjustments of the simulation program. After which the second period can be used as a control. For this work it would mean that we should in fact use a new period as a control, because the February period had excessive tank loss.

References

[1] Jordan, R.C. & B.Y.H. Liu (edit.):
Applications of Solar Energy For Heating and Cooling of Buildings.
ASHRAE, New York, 1977.

[2] Duffie, J.A. & W.A. Beckman:
Solar Energy Thermal Processes.
John Wiley & Sons, New York, 1974.

[3] Lawaetz, H. & S. Svendsen:
Termisk Effektivitet af en solfanger, beregnet og målt.
Thermal Insulation Laboratory, Technical University of Denmark. Report no. 57, 1977.

[4] Jørgensen, Ove:
Modelling and Simulation. IEA task 1, subtask a report.
Thermal Insulation Laboratory, Technical University of Denmark, October 1979.

[5] Balcomb, J.D., J.C. Hedstrom and H.S. Murray:
Solar Heating and Cooling Performance of the Los Alamos National Security and Resources STUDY CENTER.
CCCMS/ISES Conference, Dusseldorff, 1978.

[6] Hollands, K.G.T. et al.
Free Convective Heat Transfer Across Inclined Air Layers.
Journal of Heat Transger, 1976.

[7] Kennish, W.J.:
Validation format for the comparison of hourly simulation and experimental data.
TPI, Energy Systems Analysis
USA, 1979.

[8] Meinel, A.B. & M.P. Meinel:
Applied Solar Energy.
University of Arizona, 1976.

APPENDIX A

The SVS-Program

A.1 Short description of the SVS-program.

The SVS-program is illustrated by two flowcharts in this appendix, where there is also a short description of the most important subroutines.

The data from the Study Center (see p. 6) is read by the subroutine DISKQ. From DISKQ the common block /KORS/ with the input data are transferred to the subroutines SOL and STYR. SOL and SUNR are used to calculate weather data and the common block /VEJR/ from SOL and SUNR is also transferred to STYR. In the SVS-program are also included subroutines to calculate the sun's radiation, and the heating demand for a building, but this is not necessary in validation work where these values are measured, and used as input data. The subroutine STYR calculates all the heat flows and temperatures in the solar heating system, and calls the solar collector subroutine OPFA every hour to calculate the solar collector.

When you shall make calculations of different solar systems with the SVS-program, you will have to put the system parameters into the program in two different ways. First it is possible to change parameters by using the data-name AKORT(I,J). For instance, you can change the collector m^2 by changing AKORT (I,J) see page 90. Second you will have to make changes in STYR, if there is other parameter changes than those described by AKORT(I,J). In the Study Center Validation work we had to make changes in STYR.
For further reading ref. [3] and ref. [4].

On the following pages of this appendix there is a description of the SVS simulation code, taken from the IEA task 1, subtask A report: "Modelling and Simulation", third draft November 1978:

Description of the S.V.S. simulation code.

Introduction.

This program, which is developed at the Thermal Insulation Laboratory at the Technical University of Denmark, is based upon programs developed for the Zero-Energy-House by T. Esbensen and for solar heating systems by H. Lawaetz.

The program consists of a number of subroutines, which either model components or have mathematical functions. The program is quasi-stationary, meaning that energy flows within the timestep are supposed to be stationary.

Description of the computer model.

The program calculates the entire system every hour or half hour in a year, and after that a test is made upon the storage temperature. If it deviates less than $1^{o}C$ from the start storage temperature the computation is stopped. Otherwise the calculation continues month by month until the storage temperature deviates less than $1^{o}C$ from the temperature at the same time last year. The system in that way is in balance with the climatic data and the heat loads, so a continued calculation does not give results which differ from those last year.

The computing time will be about 1 min. for the solar water system and about 2 min. for the solar air system.

The computation is carried out by an IBM 370/165 system, compiled by a FORTG compiler. Core needed approx. 58 k + input-output buffers, total 82 k.

Depending how the climatic data and house loads are available (explained in section "Input data") the structure of the programs ready for computation may look as shown in the flowchart.

Fig. 1. Flowchart for MAIN

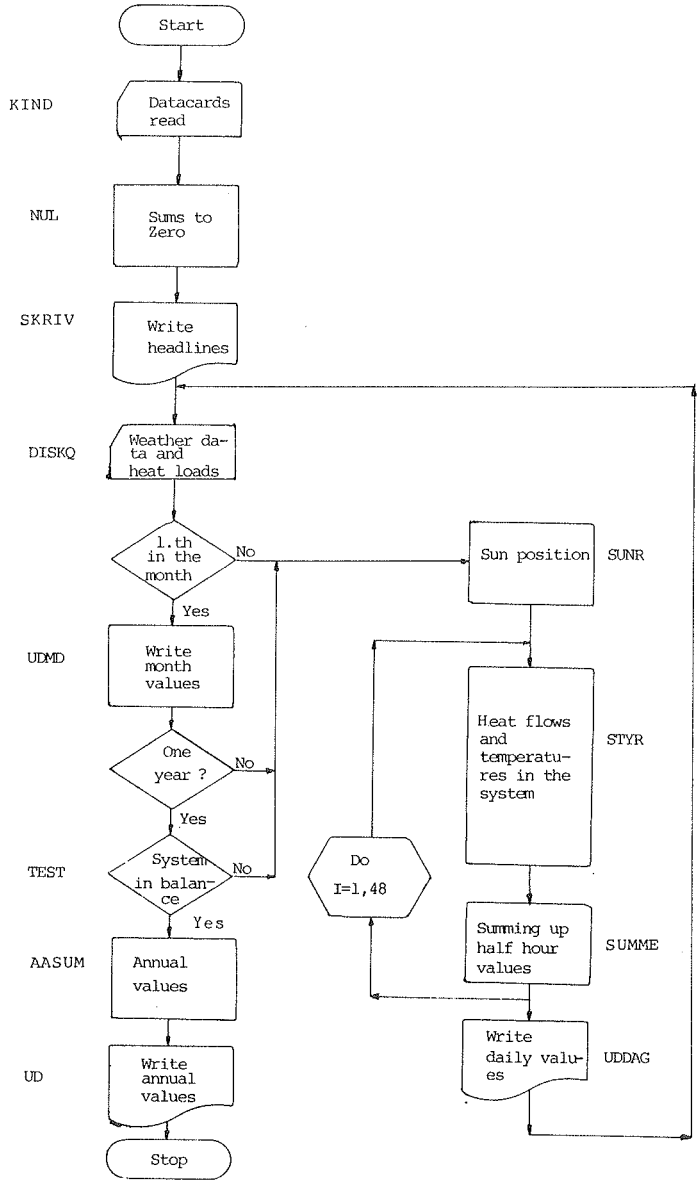

The subroutine STYR controls the energy transports (heat flows) and calculates the temperatures of the system. At the moment four different STYR-subroutines exist at the laboratory for as many different solar heating systems:

1) Combined heating and PHW liquid system.
2) Combined heating and DHW air system.
3) Combined solar heating and heat pump system.
4) Liquid DHW system.

A special subroutine for calculating the pebble bed storage has been developed for the air system.

The subroutine OPFA calculates the energy gain by the solar collector. Five different subroutines exist at the laboratory, two for a one glazed water-based collector, two for a two glazed water-based collector and one for a two glazed air based collector.

Only the key subroutines used in the IEA-simulations will be described here.

Subroutine STYR for a water system.

1) At the first call the geometric parameters, the heat contents in the tanks and the heat loss coefficient are calculated.
2) The collector is calculated by calling the collector the collector subroutine.
3) The heat transported to the storage and the new temperatures of the collector circuit pipings are calculated.
4) Calculations of heat moved from storage to preheat tank by a heat exchanger and heat needed for domestic hot water from the preheat tank.
5) Calculation of heat needed for house heating from storage to house air through the coil.
6) Calculations of heat losses from the system and new temperatures in the heating circuit pipings.
7) Calculations of the new temperatures of the storage tank and the preheat tank.

Fig. 2. Flowchart for STYR (water system)

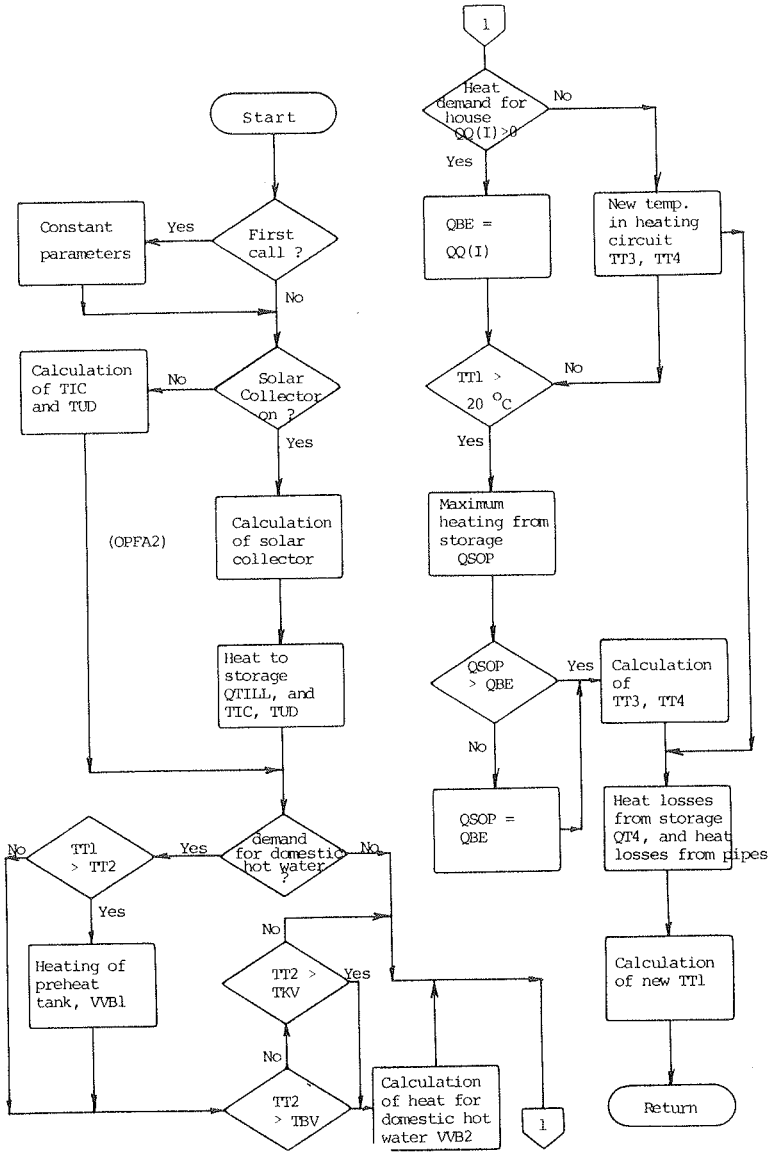

TBV Needed temperature for domestic hot water.
TT2 Temperature of preheat tank.
TT1 Temperature of storage tank.
TIC Inlet temperature to collector.
TUD Outlet temperature from collector.
QTILL Solar heat to storage.
VVB1 Heat from storage to preheat tank.
VVB2 Heat from preheat tank to domestic hot water.
QQ(I) = QBE, Heating demand of the house.
TT4 Temperature in the heating circuit from storage.
TT3 Temperature in the heating circuit to storage.
QSOP Solar heating from storage.
QT4 Heat loss from storage.
TKV Temperature of cold water from mains.

Fig. 3. AKORT (I.J.) for the SVS-program.

I \ J	1	2	3	4	5	6	7	8
1	Solar collector	Collector area	Tilt	Orientation from south	Reflection coeff. of surround.	OPFA1 = 1 OPFA2 = 2	Latitude	Longitude	Local time
2	Storage tank (I)	Volume	Insulation (m)	Start temperature	Temperatur of surround.	Max. temperature			
3	Preheat tank (II)	- " -	- " - (m)	- " -	- " -				
4	Heat exchanger (I)	Heat transfer coefficient ($W/^oC, m_c^2$)	Fluid flow (Collector) ($l/min, m_c^2$)	Fluid flow (2 side) ($l/min, m_c^2$)	Pump start temperature, diff. (abs.storage)	Min. Δ T in collector to run the pump			
5	Heat exchanger (II)	- " - ($W/^oC$)	- " - L/s	- " - L/s					
6	Domestic hot water	Demand L/day	Hot water temperature (^oC)	Cold water temperature (^oC)		1			
7	Start day	Start day	Number of days	TSTEP					
8	Data out		--------	Days for	half-hour	values tables	-------		
10	Domestic hot water tank	Volume (c)	Insulation (m)	Temperature of surround.					
11	Building heating	Heat demand (W)	Heating temperature of fluid (^oC)	Return temp. of fluid (^oC)	Room temperature	Heating fluid flow $6/min, m_c^2$	Max. air flow to room		

A.2 The SVS Simulation of the Los Alamos Study Center solar heating system.

For each timestep TSTEP the direct and diffuse solar insolation, Q35,D = DIR and Q35,I = DIF are calculated as on page 4. Then the solar collector subroutine is called, if the sun is up and if TC1 is less than 95 ^{o}C. Output from the collector subroutine is QSOL. T_1 and QA2.

In the validation work with the Study Center results, we have used two different kinds of STYR-versions. In the number two version which is used for the December calculation we have introduced a new way to calculate pipe losses (see page 79), and also a new way to control the collector circuit pump. (This is illustrated at the flow-chart in fig. 4).

When the pump is on, the fluid mass flow, FLOW, is calculated as a function of TC1 from the previous hour, and the temperatur rise over the collectors, DTAF is now calculated as:

$$DTAF = TC2 - TC1 = (QSOL * F''')/(\dot{m}_s \cdot C_{p,s})$$

then we also have the inlet and outlet temperatures of the collectors.

$$TC1 = TS1 + DTAF \frac{1}{\epsilon_{vv}} - 1$$

$$TC2 = TC1 + DTAF$$

see also fig. 5 page 22.

Flow chart of pump control

Fig. 4.

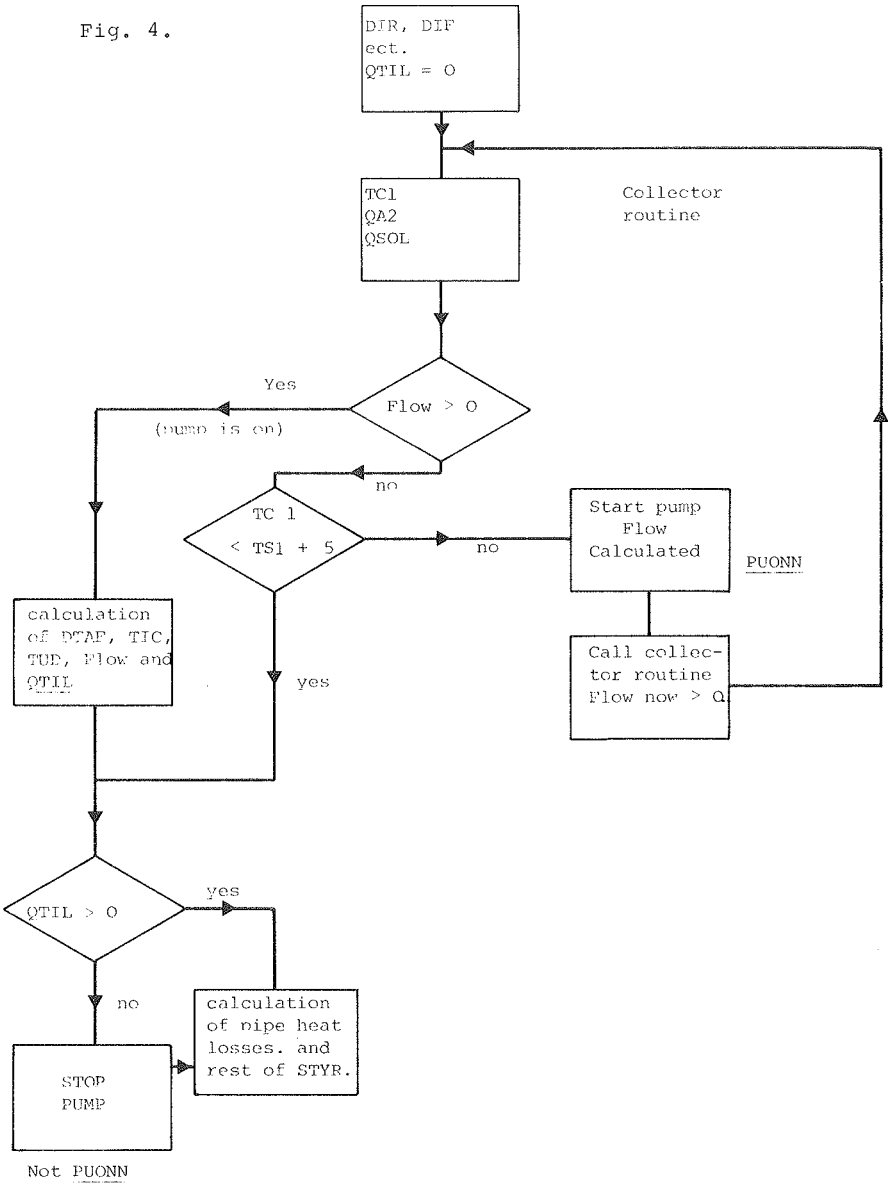

Now the energy leaving the collector, QTIL, is calculated as:

QTIL = QSOL * F''' * AR1 * TSTEP (J)

Calculation of pipe heat losses in the collector circuit is done in three different ways: starting up, when pump is on and when pump is off (see fig. 5).

Fig. 5. The collector circuit.

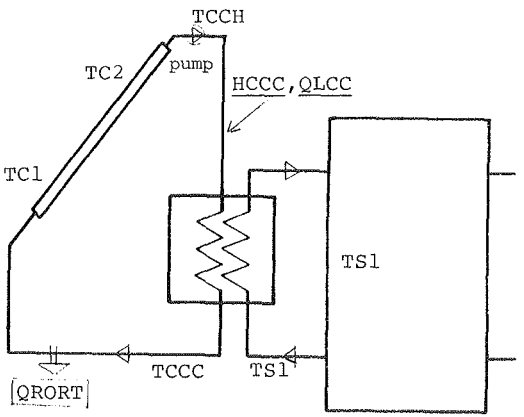

(TOMG is temperature of surroundings)

The heat loss from the collector circuit pipes is:

$$QLCC = 0.1 * AR1 * TSTEP \quad (J/^{o}C)$$

And the heat capacity of the pipes

$$HCCC = 5000 * AR1 \quad (J/^{o}C$$

The capacity flow of the fluid is:

$$FLOA = \dot{m}_s \cdot C_{p,s} \cdot TSTEP \quad (J/^{o}C)$$

Calculation of pipe heat loss

a) when pump is off:

$$TCCC = (TCCC - TOMG) * \exp\left(\frac{-QLCC}{HCCC}\right) + TOMG$$

$$TCCH = (TCCH - TOMG) * \exp\left(\frac{-QLCC}{HCCC}\right) + TOMG$$

$$QRORT = 0$$

b) when the pump is on, and it is the first hour after it was off:

$$QRORT = HCCC * (TC1 - TCCC + TC2 - TCCH) \quad (J)$$

here the pipe heat losses from the "pump off" period is taken into account.

c) when the pump is on, and it was also on the hour before:

$$TCCC = \frac{\left[TC1 * (FLOA - QLCC + (TOMG * QTCC)\right]}{(FLOA + QLCC)}$$

$$TCCH = \frac{\left[TC2 * (FLOA - QLCC + (TOMG * QTCC)\right]}{(FLOA + QLCC)}$$

$$QRORT = FLOA * (TC1 - TCCC + TC2 - TCCH) \quad (J)$$

From the collected solar energy QTIL, and the pipe heat loss QRORT, the solar energy entering the heat exchanger, QTILL, is calculated as:

$$QTILL = QTIL - QRORT$$

Because we do not calculate heat losses from the heat exchanger and from the heat exchanger circuit, QTILL will also be the value of the solar energy entering the storage tank.

Domestic hot water calculation

The heat demand for hot water is:

$$FVVS = DHW * TSTEP * 1000./40 \quad (J/^{o}C)$$

If TS1 is higher than the domestic hot water tank temperature TDHW, the solar heat to the hot water tank, VVB1, is calculated:

The capacity flow to the tank is:

$$FVFF = \dot{m}_{dv} * TSTEP * C_{p,v} * \rho_{v}/1000 \quad (J/^{o}C)$$

and the temperature rise of flow

$$TTRE = TDHW + \epsilon_{dv} * (TS1 - TDHW)$$

then we have

$$VVB1 = FVFF * (TTRE - TDHW) \quad (J)$$

we now calculate the heat leaving the hot water tank, VVB2

$$TDHW \geq 50\ ^{o}C: \quad VVB2 = FVVS * (50-10) \quad (J)$$

$$TDHW < 50\ ^{o}C: \quad VVB2 = FVVS * (TDHW - 10) \quad (J)$$

The heat loss from the hot water tank is calculated as.

$$QDL = UA_{DH} * (TDHW - TOMG) * 3600. * \left[1 + \frac{(TDHW - TOMG)}{265}\right] (J)$$

And the heat content in the tank:

$$QT2 = QT2 + VVB1 - VVB2 - QDL$$

Which immediately gives the new domestic hot water tank temperature TT2.

Building heating calculation

The heat demand for building heating is

QBE = QB * 1000. * TSTEP (J)

As mentioned before the building heating is controlled by a switchover temperatue T_s which is a function of ambient temperature, T_a.

When the storage temperature is higher than T_s, then solar heat should be able to provide all of the heating demand, and the solar mode, mode 1 is on.

The solar heat leaving the storage tank, QSOP, is then:

mode 1, QSOP = QBE, QAUX = 0
mode 2, QSOP = 0, QAUX = QBE

The heat loss from the storage tank is

$$QTL = UA_{ST} * (TS1 - TOMG) * TSTEP * \left(1 + \frac{(TS1 - TOMG)}{265}\right) \quad (J)$$

$$, UA_{ST} = 0.64 * 71.5 = \underline{45.76\ W/^{o}C}$$

The heat loss from the pipes of the building heating circuit is calculated as a heat loss from the storage tank.

The capacity flow of the water in the building heating circuit is

$$FLOAH = \dot{m}_{b,v} * AR1 * C_{p,v} * \rho_v * TSTEP/1000. \quad (J/^{o}C)$$

The heat loss from the building heating pipes is

$$QLHC = 0.15 * 20 * TSTEP \quad (J/^{o}C)$$

And the heat capacity of the pipes

$$HCHC = 2160 * 20 \quad (J/^{o}C)$$

Fig. 6. The hot water and building heating circuit.

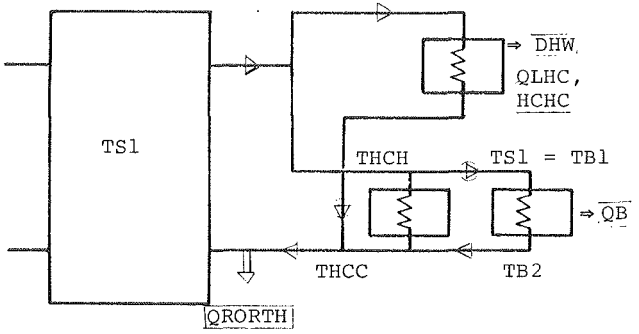

When the pump in the building heating loop is on, the temperature of the water leaving the storage tank TB1 is TS1, and the temperature of the water leaving the building heating system TB2 is then.

TB2 = TS1 - QSOP/FLOAH

The temperature of the hot side of the pipes is called THCH and of the cold side THCC, now we can calculate the heat losses from the pipes QRORTH:

a) when the pump is off:

$$THCC = (THCC - TOMG) * \exp\left(\frac{-QLHC}{HCHC}\right) + TOMG$$

$$THCH = (THCH - TOMG) * \exp\left(\frac{-QLHC}{HCHC}\right) + TOMG$$

QRORTH = 0

b) when the pump is on, and if it is the first hour after it was off:

QRORTH = HCHC * (TB2 - THCC + TB1 - THCH) (3)

here the pipe heat losses from the "pump off" period e.g. the night) is taken into account.

c) when the pump is on, and it was also on the hour before.

$$THCC = \frac{TB2 * (FLOAH - QTHC + (TOMG * QTHC)}{FLOAH + QUHC}$$

$$THCH = \frac{TB1 * (FLOAH - QTHC + (TOMG * QTHC)}{FLOAH + QTHC}$$

$$QRORTH = (TB2 - THCC + TB1 - THCH) * FLOAH \quad (J)$$

Now we can calculate the heat in the storage tank QT1, as:

$$QT1 = QT1 + QTILL - QTL - VVB1 - QSOP - QRORTH$$

and we also get the new storage temperature TS1.

TS1 is then the new value of TIND to calculate the solar collector.

A.3 Calculation of the Solar Collector

Input parameters to the collector calculation subroutine which are called every hour when the sun is up

TCl	temperature of fluid entering the collectors	(^{o}C)
$\dot{m}$	mass flow in collector circuit	(kg/h)
TILT	angle of collector	
VINK	angle of incidence	
DIR	direct insolation	(W/m^2)
DIF	diffuse insolation	(W/m^2)
T_a	ambient temperature	(^{o}C)
V	wind speed	(m/s)
T_s	sky temperature	(^{o}C)

Other parameters used in the collector calculation

τ_c	calculated tranmission	
h	heat loss coefficient	(W/m^2 ^{o}C)
σ =	5.67×10^{-8}, Bolzmans constant	
T_1	temperature of absorber	(^{o}C)
T_2	temperature of cover	(^{o}C)
ϵ_g =	0.88 Emission coefficient of glass	
QA2	absorbed solar heat	(W/m^2)
ABSll	heat absorbed by cover	(W/m^2)
$\dot{m}$	mass flow of collector fluid	(kg/h)
C_p	heat capacity of fluid	(J/kg ^{o}C)
F'	collector factor	
F''	flow factor	
QSOL	collector output, (which does not take the heat exchanger in account).	(W/m^2)

The Collector Calculation:

For the insolation reaching the solar collector we have

The angle of refraction i_b

$$i_b = \arcsin(\sin(i_i)/n) \tag{1}$$

i_i is angle of incidence, and n the retractive index.

From Fresnels formula we get the reflection coefficients:

$$r_1 = \frac{\sin^2(i_i - i_b)}{\sin^2(i_i + i_b)} \tag{2a}$$

which is the fraction reflected in the plane perpendicular to the plane of incidence.

$$r_2 = \frac{tg^2(i_i - i_b)}{tg^2(i_i + i_b)} \tag{2b}$$

which is the fraction reflected in the plane parallel to the plane of incidence.

From this we get the transmittance coefficient, with only reflection taken in account.

$$\tau_r = 0.5 \times \frac{1-r_1}{1+r_1} + \frac{1-r_2}{1+r_2} \tag{3}$$

The thickness of the glass cover is E, then the insolation lenght through the glass will be:

$$L = \frac{E}{\cos i_b} \tag{4}$$

We now get the transmittance coefficient, with only absorption taken in account.

$$\tau_a = e^{-K \cdot L} \tag{5}$$

K is the extension coefficient for the glass.

The total transmission is now:

$$\tau = \tau_r \cdot \tau_a \tag{6}$$

Some of the insolation reaching the absorber is absorbed, and some is reflected to the cover, where a fraction is transmitted, and a fraction is reflected to the absorber again. The reflection coefficient of glass at a mean incidence of insolation of 60^{o} is: $\rho_{i=v} = 0.16$. We now use the following equation for the effective transmissivity-absorptivity product $(\tau\alpha)_e$:

$$(\tau\alpha)_e = (\tau\alpha)_t + (1-\tau_a)\cdot All \qquad (7)$$

where All is 0.13 for a selective surface,

$(\tau\alpha)_t$ is the $(\tau\alpha)$ product for the primary insolation:

$$(\tau\alpha)_t = \frac{\tau\cdot\alpha}{1 - (1-\alpha)\cdot\rho_{i=v}} \qquad (8)$$

For all the expressions mentioned above we make two calculations, one for direct insolation and one for diffuse insolation. To calculate the diffuse insolation we use an angle of incidence of 50^{o}, while for the direct insolation we use the actual value of the angle of incidence. We use the following indices for the two types of insolation:

direct insolation:	d
diffuse insolation:	i

Calculation of the Collector Heat Loss

1. Heat loss from absorber to cover

   a. Radiation heat loss from absorber to cover is given by:

$$h_{r,1} = \frac{\sigma\cdot(T_2^2 + T_1^2)(T_2 + T_1)}{1/\varepsilon_g + 1/\varepsilon_p - 1} \qquad (9)$$

   b. Convection from absorber to cover:

$$h_{c,1} = PB\cdot(9/5)\cdot|(T_2 - T_1)|^{0.25}$$

$$\text{where } PB = (0.24 - TILT/1000)\cdot 5.67 \qquad (10)$$

2. Heat loss from cover to the ambient

a. Radiation from cover to the sky:

$$h_{r,2} = \varepsilon_g \cdot \tau \cdot (T_1^2 + T_s^2)(T_1 + T_s) \qquad (11)$$

where T_s is given by the expression:

$$T_s = 1.15 \cdot T_a - 46 - 9 \cdot \cos(TILT)$$

b. Convection from cover to the surroundings by wind:

$$h_{c,2} = 5.7 + 3.8 \cdot V \qquad (12)$$

The above calculated heat losses are illustrated in figure 7:

Fig. 7

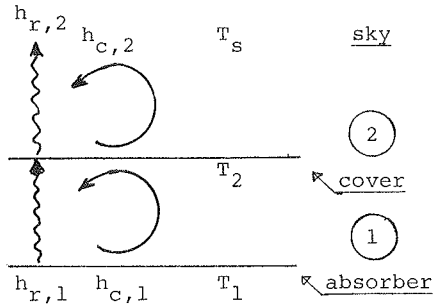

The total heat loss from the collector cover is now given by:

$$h_c = \left(\frac{1}{h_{c,2} + h_{r,2}} + \frac{1}{h_{c,1} + h_{r,1}} \right)^{-1} \qquad (13)$$

The effective $(\tau\alpha)$ product we have from equation (7) for direct and indirect insolation, $(\tau\alpha)_{e,d}$ and $(\tau\alpha)_{e,i}$.

Calculation of heat absorbed by the cover and by the plate.

The transmission coefficient of the primary insolation is given by:

$$\tau_p = \frac{(\tau\alpha)_{t,d} + (\tau\alpha)_{t,i}}{\alpha}$$

and for the total insolation (both primary and secondary):

$$\tau_e = \frac{(\tau\alpha)_{e,d} + (\tau\alpha)_{e,i}}{\alpha}$$

Now we can calculate the coefficient for the heat which is absorbed by the cover. This is the difference between the total transmission coefficient and the primary transmission coefficient.

$$\alpha_g = \tau_e - \tau_p = \frac{1}{\alpha} \cdot ((\tau\alpha)_{e,d} - (\tau\alpha)_{t,d}) + ((\tau\alpha)_{e,i} - (\tau\alpha)_{t,i})$$

Iteration process to find T_1, T_2, h_c and QSOL:

To find the unknown parameters T_1, T_2 and h_c, we make an iterative process where we start with a guess of the plate temperature T_1 = TC1 (the collector inlet temperature) and the cover temperature $T_2 = T_a$ (the ambient temperature). But first we must find some other values which we need to make the necessary heat balances of the collector cover and the collector plate.

When we use equation (7).

$$\alpha_g = \frac{All}{\alpha} \cdot \left[(1 - \tau_{a,d}) + (1 - \tau_{a,i})\right]$$

and now we have the heat absorbed in the cover.

$$ABS11 = \frac{All \cdot 0.98}{\alpha} \cdot \left[(1 - \tau_{a,d}) \cdot DIR + (1 - \tau_{a,i}) \cdot DIF\right] \quad (14)$$

We now get the heat which is absorbed by the absorber plate as:

$$QA2 = 0.98 \cdot ((\tau\alpha)_{e,d} \cdot DIR + (\tau\alpha)_{e,i} \cdot DIF) \quad (15)$$

The F' factor for the collector we assume to be 0.95 (15)

and the total heat loss coefficient we find by calculating the side heat loss as 5% of the front heat loss. The back heat loss comes from heat conduction: (λ_b/D_b), where λ_b is

the conduction coefficient of the insulation material, and D_b is the thickness. Then the total heat loss coefficient U_L is

$$U_L = 1.05 \cdot h_c + (\lambda_b / D_b) \tag{16}$$

The F" factor which is also called the collector flow factor we find as:

$$F'' = \frac{\dot{m} \cdot C_p}{U_L \cdot F'} \cdot \; 1 - e - \left(\frac{U_L \cdot F'}{\dot{m} \cdot C_p}\right) \tag{17}$$

where $\dot{m}$ is the mass flow in the collector circuit.

Now we are able to find the plate temperature T_1, because we know that the total heat loss from the plate is the same as the difference between the absorbed heat at the plate and the useful heat which leaves the collector.

$$(T_1 - T_a) \cdot h_t = QA2 - F' \cdot F''(QA2 - (h_t \cdot ABS(TC1 - T_a)))$$

which is equal to:

$$T_1 = T_a + \frac{1}{U_L} \cdot (QA2 - F' \cdot F''(QA2 - (U_{L2} \cdot ABS(TC1 - T_a)))) \tag{18}$$

To find the cover temperature T_2 we will use a heat balance of the cover. The heat leaving the cover is equal to the convection and radiation heat loss to the ambient, and the heat coming to the cover is equal to the heat gain by radiation and convection from the absorber, plus the absorbed heat in the glass ABS11 (see fig. 8). This means:

$$h_{c,2} \cdot (T_2 - T_a) + h_{r,2} \cdot (T_2 - T_s) - (h_{c,1} + h_{r,1}) \cdot (T_1 - T_2) - ABS11 = 0$$

Fig. 8.

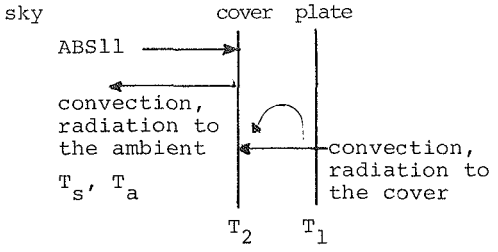

which is the same as:

$$T_2 = (h_{c,2} \cdot T_a + h_{r,2} \cdot T_s + (h_{r,1} + h_{c,1}) \cdot T_1 + ABS11)$$

$$/(h_{c,2} + h_{r,2} + h_{c,1} + h_{r,1}) \qquad (19)$$

When the results of the iteration process, T_2 and T_1 are as near the input T_2, T_1 (which we got from the last run) as $0.1^{o}C$, we conclude that T_2 and T_1 now have been found. That means that we also have the value of U_L.

Now we know the amount of heat that will be gained from the sun in the collectors, QSOL:

$$QSOL = F' \cdot F'' \cdot (QA2 - U_L(TC1 - T_a)) \qquad (20)$$

Output of collector calculations are:

QSOL, T_1 and QA2

These parameters are used in the subroutine which calculates the rest of the solar heating system, called STYR.

References to the collector calculations, where you can find all equations used are [1], [2] and [3].

A.4 Parameter names in the SVS-program

The parameter names used in this report are not quite the same as the parameter names which you will find in the SVS-program. Below is a list where the names used here are translated into SVS-names:

COLLECTOR SUBROUTINE

	Report name	SVS-name	
collector area	m_c	AR1	(m^2)
tilt	TILT	TILT	
glass transmission (measured)	τ_c		
glass transmission (calculated)	τ_g	T1D1	
glass thickness	E	B1	
refractive index	n	BIX	
extinction coeff.	K	A	
absorptivity (absorber)	α	ALFA	
emissivity (absorber)	ε_p	EPSC	
insulation thickness	D_b	DI	(m)
insulation conductivity	λ_b	LAMDA	(W/m^oC)
shade factor	SFAK	SFAK	
collector inlet temperature	TC1	TIC	(^oC)
mass flow in collectors	$\dot{m}$	G,FLOW	(kg/h)
angle of collectors to south	VINK	VINK	
ambient temperature	T_a	UDT	(^oC)
wind speed	V	V	(m/s)
sky temperature	T_s	TS	(^oC)
heat loss coefficients:	$h_{c,1}$	HC1	($W/m^{2o}C$)
	$h_{r,1}$	HRC1	-
	$h_{c,2}$	HW	-
	$h_{r,2}$	HR1S	-
	h_c	UUP2	-
	U_L	UL2	-
absorber temperature	T_1	TC1	(^oC)
cover temperature	T_2	TG11	(^oC)

	Report name	SVS-name
emission coeff. of glass	ε_g	EPS1
absorbed solar heat	QA2	QA2 (W/m^2)
heat absorbed in cover	ABS11	ABS11 (W/m^2)
heat capacity of fluid	C_p	CP (J/kg^oC)
collector factor	F'	FM2
flow factor	F"	FMM2
collector output (without heat exchanger)	QSOL	QSOL,QU2 (W/m^2)
angle of refraction, direct	$i_{b,d}$	BR
diffuse	$i_{b,i}$	BRD
angle of incidence, direct	$i_{i,d}$	VINK
diffuse	$i_{i,i}$	50^o
reflection coeff., direct	$r_{1,d}$	R1
diffuse	$r_{1,i}$	RD1
direct	$r_{2,d}$	R2
diffuse	$r_{2,i}$	RD2
transmittance coef. (direct)	$\tau_{r,d}$	0.5(TR1+TR2)
diffuse	$\tau_{r,i}$	0.5(TRD1+TRD2)
direct	$\tau_{a,d}$	PA1
diffuse	$\tau_{a,i}$	PAD1
direct	$\tau_{t,d}$	T11
diffuse	$\tau_{t,i}$	T1D1
insolation length in glass, direct	L_d	B (m)
diffuse	L_i	BD (m)
($\tau\alpha$) products (direct and duffuse)	$(\tau\alpha)_t$	FC FC1D
	$(\tau\alpha)_e$	FE1 FE1D
reflection coeff.	$\rho_{i=v}$	0.16
constant	A11	0.13

STYR SUBROUTINE

	Report name	SVS-name	
collector inlet temperature	TC1	TIC	(^{o}C)
collector outlet temperature	TC2	TUD	-
heat exchanger inlet temperature	TC3		-
heat exchanger outlet temperature	TC4		-
collector pipe temperature, cold side	TCCC	TCCC	-
collector pipe temperature, hot side	TCCH	TCCH	-
heat capacity of collector pipes	HCCC	HCCC	(J/^{o}C)
heat loss from collector pipes	QLCC	QTCC	(J/^{o}C)
heat capacity of collector fluid	$C_{p,s}$	1970	(J/kg ^{o}C)
density of collector fluid	ρ_s	857.5	(kg/m^3)
mass flow of collector fluid	$\dot{m}_s$	FLSO	(kg/s)
mass flow of collector fluid per m^2		FLOW	(kg/s,m^2)
heat capacity of water	$C_{p,v}$	4179	(J/kg ^{o}C)
density of water	ρ_v	996	(kg/m^3)
mass flow of water in heat exchanger circuit	$\dot{m}_{v,v}$		(kg/s)
heat leaving the collector	QTIL	QTIL	(J)
heat entering the heat exchanger	QTILL	QTILL	(J)
storage tank temperature	TS1	TT1	(^{o}C)
heat transfer coefficient of the heat exchanger	U_H		(W/^{o}C)
efficiency of heat exchanger	ϵ_{vv}	0.37	
heat exchanger factor	F'''	0.92	
storage heat loss	$U_{L,S}$	45.76	(W/m^2 ^{o}C)
domestic hot water flow	$\dot{m}_{d,v}$	0.95	(kg/s)
building heating circuit flow	$\dot{m}_{b,v}$	3.78	(kg/s)
direct sun insolation	DIR	DIR	(W/m^2)
diffuse sun insolation	DIF	DIF	(-)
rise in temperature in collector	DTAF	DTAF	^{o}C
capacity flos of fluid in collector circuit	FLOA	FLOA	(J/^{o}C)
temperature of surroundings	TOMG	21.1 ^{o}C	
heat loss from pipes in collector circuit	QRORT	QRORT	(J)
heat demand for hot water	FVVS	FVVS	(J/^{o}C)

	Report name	SVS-name	
temperature in domestic hot water tank	TDHW	TT2	(^{o}C)
capacity flow to hot water tank	FVFF	FVFF	(J/^{o}C)
temperature rise	TTRE	TTRE	(^{o}C)
timestep	TSTEP	TSTEP = 3600 s	
heat leaving domestic hot water tank	VVB2	VVB2	(J)
heat loss from domestic hot water tank	QDL	QT5	(J)
heat transfer in DHW-tank	U_{DHW}	2035	
heat in DHW-tank	QT2	QT2	
heat capacity of DHW-tank	HT	1582	(kJ/^{o}C)
heat demand for building heating	QBE	QBE	(J)
solar heat for building heating	QSOP	QSOP	(J)
storage tank loss	QTL	QT4	(J)
heat loss coefficient of storage tank	UA_{st}	45.76	(W/^{o}C)
capacity flow of water in building heating circuit	FLOAH	FLOAH	(J/^{o}C)
heat loss from BH-circuit pipes	QRORTH	QRORTH	(J)
heat loss coefficient from BH-circuit pipes	QLHC	QLHC	(J/^{o}C)
heat capacity of BH-pipes	HCHC	HCHC	-
temperature f water leaving storage	TB1	TS1	(^{o}C)
temperature of water leaving BH-system	TB2		(^{o}C)
BH - pipe temperature, cold side	THCC	THCC	(^{o}C)
BH - pipe temperature, hot side	THCH	THCH	(^{o}C)
heat in storage tank	QT1	QT1	(J)
heat capacity of storage tank	HCST	157.542	(kJ/^{o}C)
solar circuit pump on		PUONN	
solar circuit pump on last hour		PUONF	
heating circuit pump on		PHONN	
heating circuit pump on last hour		PHONF	
% solar		SEF	

APPENDIX B

The Los Alamos Study Center solar heating system.

SOLAR HEATING AND COOLING PERFORMANCE OF THE LOS ALAMOS NATIONAL SECURITY AND RESOURCES STUDY CENTER

by

Hugh S. Murray, James C. Hedstrom and J. Douglas Balcomb
Los Alamos Scientific Laboratory
P. O. Box 1663
Los Alamos, New Mexico 87544 U.S.A.

SYSTEM PERFORMANCE

I. GENERAL DESCRIPTION OF SYSTEM PROJECT AND EQUIPMENT

A. Objective of Project

The National Security and Resources Study Center (NSRSC) at The Los Alamos Scientific Laboratory (LASL), Los Alamos, New Mexico, is a unique building which has a solar heating, ventilating, and air conditioning system developed by LASL's solar energy group. Funded by the Department of Energy as part of the building construction budget, the solar system is designed as a continuing research project which will provide data needed in the design of energy saving systems for commercial buildings.

The building makes use of many energy conserving features combined with the solar energy system. Sufficient instrumentation has been installed in the building to permit the monitoring of energy production and consumption in all of the modes of operation. A computer controls the data acquisition and processing. Experiments planned for the NSRSC include solar energy system performance and system optimization studies. It is planned to complete the performance studies by October, 1978.

B. Description of the Environment

1. Climate

Los Alamos has a semiarid continental mountain climate. Maximum summer temperatures reach 32°C on an average of only two days a year. Low readings in July average around 10°C. Winters are cold, with night time temperatures below freezing from November through mid-April. The average annual precipitation is 457 mm of rain and 1270 mm of snow.

Most winter days are clear and sunny and daytime warming is rapid. This area can expect about 70 percent of the year's possible sunshine.

*Work performed under the auspices of the U. S. Department of Energy, R & D Branch for Heating and Cooling, Office of the Assistant Secretary for Conservation and Solar Energy.

2. Location

The project is located at 35°52' north latitude, 106°19' west longitude at 2190 m above sea level. The site is located on the eastern slope of the Jemez mountains about 16 km west of the Rio Grande river, surrounded by rough, mountainous, and partially wooded country. Eastward, the terrain slopes rapidly down to the river; westward, the Jemez mountains rise to peaks above 3350 m. Air quality is good with negligible pollution. Some dust is evident during periods of strong winds in the spring.

3. Solar Radiation

Mean daily monthly solar radiation, in MJ/m^2 day, is given in Table I. These data were obtained for the year 1972-1973 on a 45° tilted, south facing surface.

TABLE I. MONTHLY SOLAR RADIATION

Jan	Feb	Mar	Apr	May	June	Jul	Aug	Sept	Oct	Nov	Dec
17.8	18.2	17.4	21.1	18.6	21.9	17.4	19.4	20.4	14.7	16.5	15.2

4. Ambient Temperatures

The monthly average dry-bulb temperature and the degree days of heating (based on 18.3°C) are given in Table II for the year 1972-1973.

TABLE II. AVERAGE DRY BULB TEMPERATURE AND HEATING DEGREE DAYS (°C)

	Jan	Feb	Mar	Apr	May	June	Jul	Aug	Sept	Oct	Nov	Dec
Temp.	-3.6	-1.5	.6	4.2	11.8	16.2	17.5	17.9	14.1	8.7	-.9	-2.5
D-Days	680	554	550	423	202	64	27	14	127	298	578	646

5. Wind

Average wind data are not available, but normally, winds are light, with moderately strong winds in the late winter and spring.

C. Description of the System

1. Qualitative Description

The building is shown in Figure 1, and a schematic of the energy and HVAC system is shown in Figure 2. The 716 m^2 collector array is seen in Fig. 1 to be structually integrated into the building, forming the roof of the mechanical equipment room. Architecturally, the single collector array is used to enhance the appearance of the building and not give the impression of an "add-on" solar energy system. The total air-conditioned floor area of the building is 5574 m^2 on three floors. The lower floor contains the report library, the ground floor contains the main library, and the upper floor houses two meeting

rooms, offices, and several smaller conference areas. The enclosed bridge, seen in Fig. 1, connects the NSRSC with the main Administration Building of LASL.

The building was designed with energy conservation as the primary objective. The building shell is heavily insulated, having an overall loss coefficient of .51 $W/m^2°C$, and the HVAC system makes use of air recirculation, heat recovery, and complete shut down at night.

The HVAC system is a two-zone (perimeter and interior) variable air volume system with separate supply fans and cooling coils for each zone. The terminal boxes in the perimeter zone only have hot water reheat coils. Most of the heat in the building is provided by the people and lights, so that the interior zone, being isolated from the outside walls, requires only cooling throughout the year.

The air handling system features recirculation of inside air, and a heat-pipe heat recovery unit in the perimeter zone system serves two functions: to preheat outside air in the heating mode; and, by means of spraying the exhaust air, to precool outside air in the cooling mode. The light fixtures are cooled by the return air, and separate return fans are provided for each of the zones. The total fan flow rate for both zones is 24.4 m^3/sec, with roughly half going to each zone.

The main air supply boxes in the mechanical equipment room each have a cooling coil, air washer unit, and a supply fan. The two sets of cooling coils both receive chilled water from the main chilled water supply line coming from the chiller.

The energy system consists of the solar collector array and heat exchanger, two storage tanks, and two water chillers - a lithium-bromide absorption chiller, and an experimental Rankine cycle unit. The two water chillers will be used in a comparative study of solar air conditioning. In the heating mode, a 38 m^3 tank is used to store hot water for heating. In the cooling mode, a 19 m^3 pressurized tank is used to store solar hot water to operate either of the chillers, and cold water is stored in the 38 m^3 tank. Cold water is generated either from one of the chillers, or by night time evaporative cooling with a 31.5 l/sec cooling tower. The cooling tower is normally used to reject heat from the chillers.

The energy system is backed up by auxiliary steam heat exchangers which generate hot water directly for heating or to power the absorption chiller. Domestic hot water is generated by means of a 379 l tank connected to the large tank in the winter or to the smaller tank in the summer. An electrically heated 151 l tank is used downstream of the solar tank to augment the domestic hot water supply.

2. Quantitative Description

The collectors are fabricated of mild steel, have a selective surface of black chrome, and are single-glazed with water-white glass. 407 collectors are connected in parallel to

form the array. The collectors are cooled with a light paraffinic oil heat transfer fluid at a flow rate of 25.2 l/sec. The panels are backed with foam insulation and a metal fire barrier. A shell and tube heat exchanger provides the energy transfer to water, the working fluid of the energy system. The collector array is inclined 35° from the horizontal, and the building and array face 13° east of south.

The heating and cooling system of the NSRSC operates in two basic modes which are subdivided as follows:

Winter mode - heating

- Mode 1 - normal heating
- Mode 2 - auxiliary heating

Summer mode - cooling

- Mode 3 - normal cooling
- Mode 4 - auxiliary cooling
- Mode 5 - cooling from storage
- Mode 6 - evaporative cooling of large tank

In mode 1, the large tank is used to store hot water from the solar collection system. This water is pumped to the reheat coils in the perimeter zone terminal boxes to heat the building. In mode 2, the steam auxiliary heat exchanger provides the hot water directly if the stored hot water cannot meet the heating demand of the building.

The system is arranged in the solar cooling mode such that the large tank is in series with the chiller. In mode 3, stored solar hot water is used to run the chiller which essentially "boosts" the chilled water going to the main cooling coils. In mode 4, the auxiliary heat exchanger hot water is used to run the chiller, but the storage tank is not in the loop. In mode 5, the water chiller is not operated, but the cold water in the large tank simply goes out to the main cooling coils and returns to the tank. Mode 6 is the chilling down of the large tank using the cooling tower.

The cold water cooling control sequence operates as follows. When the ventilating fans start at 6:00 A.M., chilled water from the cold tank is provided to the cooling coils if required. Auxiliary operation is not permitted if the cold tank is below 18.3°C. The chiller starts after the solar system has heated the hot storage tank to 82 °C. The chiller continues to operate until either the hot storage tank drops below 77 °C or the cold tank drops below 9 °C. This sequence provides optimum performance of the chiller system by 1) running the chiller when collectors are operating to reduce collector temperatures, 2) forcing maximum chiller operating times and minimizing cycling, 3) operating the chiller at full capacity without internal throttling in the Rankine unit, 4) prohibiting auxiliary operation until the cooling effect from the cold tank is exhausted.

The NSRSC control system is based on pneumatic components. A considerable range of flexibility in operating the system is available.

A temperature probe is affixed to the backside of the collector array as a measure of collector surface temperature. This temperature is compared with the temperature in the large tank (winter) or small tank (summer). If a 5 °C differential is detected, the solar collector coolant and hot water pumps are started and forced to run for at least 180 sec. Because the large tank is unpressurized, a tank temperature of over 93 °C will disable the solar heat collection controller.

The hot water temperature required for reheat is scheduled based on outside air temperature, with 60 °C water required for -18 °C outside temperature, and 38 °C water for 21 °C outside air temperature. If this schedule cannot be met by storage, the auxiliary system (mode 2) provides water at the required temperature.

The air volume in each terminal box is controlled locally by the associated zone thermostat. The demanded volume ranges from 50% of design at 1.1 °C below the temperature set point to full open at 1.1 °C above the set point. A status pressure probe in each main supply system is used to measure the total air volume demand and to modulate the inlet vanes on the supply and return fans to meet this demand. In the perimeter system, the zone thermostats also control the reheat coil water flow rate in the heating modes. The schedule for this function is for no hot water flow at the desired temperature to full flow at 1.1 °C or more below the set point. The zone set points are normally 25 °C except that the set point is automatically lowered to 21 °C in the perimeter zone when the changeover to the winter mode is made.

The fans are shut down completely during the night and the building is allowed to "coast". A low limit thermostat will cause the system to restart at half of design air volume if the temperature drops below 15 °C.

The main supply air temperature is controlled by selecting the individual zone for which is the warmest. In the perimeter zone in the winter mode, the lowest zone temperature controls the set point of the fan discharge temperature control system. In the summer mode, as the worst zone temperature gets higher, a lower fan discharge temperature is called for. This initiates a sequence of events as follows:

1. Fresh air dampers modulate to full open
2. Air washers start
3. Exhaust spray starts
4. Chilled water pump starts (mode 5) and the cooling coil bypass dampers modulate under discharge temperature control
5. Water chiller starts.

A relative humidity probe in each supply fan discharge region is used to regulate the main air washers. Although the system does not employ humidity control as a design feature, bypass dampers are provided to present humidities from becoming too high.

and air washer shutdown results for discharge humidities exceeding an ultimate upper limit of 60%,

The perimeter zone heat recovery unit uses the following sequence:

1. Between 45 °C and 13 °C the exhaust spray is off and the bypass closed. This is the full heat recovery region. The bypass is modulated linearly between 2 °C and 5 °C.

2. Above 13 °C the bypass is closed and the exhaust spray is on if there is any call for cooling (if the fresh air dampers are fully opened). If there is no call for cooling, neither the heat recovery unit nor the exhaust spray are used.

About 160 channels of instrumentation are installed in the building for the purpose of evaluating the system performance. Basic energy consumption measurements are made on all of the energy subsystems in the building. These measurements consist of flow rates and temperature differences. In addition, electrical power consumptions of all of the pumps and fans in the system are measured. Most temperatures are measured using platinum resistance thermometers, with some thermocouples on the collector array and the Rankine chiller. Flows are measured with turbine flowmeters and Annubar probes. A number of air flow, temperature, and humidity measurements are also made in the HVAC system. Solar flux is measured in the plane of the collector and in the horizontal plane.

Data acquisition is controlled by a PDP-11/34 computer. The computer provides the capability for real-time engineering calculations for data compression. This eliminates the necessity of storing large volumes of data for later analysis.

The computer automatically provides periodic system energy summaries for display and storage. Monthly and seasonal energy summaries are also calculated automatically.

II. SYSTEM THERMAL PERFORMANCE

A. Monthly Energy Summaries

Two months' (August and September, 1977) cooling data have been recorded from the system. The cooling system thermal performance for this period is summarized in Table III. Heating system data were recorded from November 1977 through April 1978. Heating system thermal performance is given in Table IV. The energies are mean daily values in MJ/day.

TABLE III

SOLAR COOLING SYSTEM THERMAL PERFORMANCE

	August	September
Incident Solar Energy	13405	14014
Solar Energy to Hot Storage	3566	3428
Solar Energy to Cooling	2588	2110
Auxiliary Energy to Cooling	960	165
Cold Water from Storage & Chiller	2661	1705

TABLE IV

SOLAR HEATING SYSTEM THERMAL PERFORMANCE

	Nov.	Dec.	Jan.	Feb.	March	Apr.
Incident Solar Energy	13984	12174	11438	13026	14618	17583
Solar Energy to Hot Storage	4902	4067	3779	4078	4838	4955
Energy Removed from Hot Storage	4299	3622	3253	3529	3949	4297
Solar Energy to Space Heating	4336	3493	3139	3446	4022	4325
Auxiliary Energy to Space Heating	570	1287	1936	1549	631	26
Heat Recovery Heat to Space Heating	1786	1786	1752	1771	1813	1320
Solar Energy to Service Hot Water	101	96	107	107	106	95

Figures 3,4, and 5 are bar graph summaries of the solar energy input and output, the building load, and storage and ambient temperatures for the heating season.

Table V summarizes the overall performance.

B. Record of the Quality of Thermal Performance of the System

Performance of the system has been as predicted except for a somewhat higher building heating load than expected.

C. Solar Contribution to Energy Requirements

Table VI summarizes the percent solar contribution to heating or cooling energy requirements of the system for the indicated months of operation.

		AUGUST	SEPTEMBER	NOVEMBER	DECEMBER	JANUARY	FEBRUARY	MARCH	APRIL
1	Incident Solar Energy	13405	14014	13984	12174	11438	13026	14618	17583
2	Solar Energy to Hot Storage	3566	3428	4902	4067	3779	4078	4338	4955
3	Energy Removed From Hot Storage	2588	2110	4299	3622	3253	3529	3949	4297
4	Solar Energy to Space Heating	0	0	4336	3493	3139	3446	4022	4325
5	Aux. Energy to Space Heating	0	0	570	1287	1936	1549	631	26
6	Heat Recovery to Space Heating	-		1786	1786	1752	1771	1813	1320
7	Solar Energy to Service Hot Water	-	-	101	96	107	107	106	95
10	Solar Energy to Cooling	2588	2110	0	0	0	0	0	0
11	Aux. Energy to Cooling	960	165	0	0	0	0	0	0
12	Energy to Cold Stor. & Building	1923	1354	0	0	0	0	0	0
13	Useful Energy From Cold Storage and Chiller	2661	1705	0	0	0	0	0	0
14	Percent of Heating and Service Hot Water From Solar	-	-	88	74	62	69	86	99
15	Percent Cooling From Solar	73	93	0	0	0	0	0	0
16	Percent Heating and Cooling From Solar	73	93	88	74	62	69	86	99
17	Electrical Energy to Pump and Fans	-	-			281	296	299	305
18	Number of Operational Days	31	30	28	31	31	28	31	30

TABLE II. SYSTEM THERMAL PERFORMANCE STUDY,
MEAN DAILY ENERGY MJ/DAY

TABLE VI

SOLAR ENERGY CONTRIBUTION

	Aug.	Sept.	Oct.	Nov.	Dec.	Jan.	Feb.	Mar.	Apr.
Percent Solar Heating or Cooling	75	92	--	88	74	63	69	86	99
Overall		81				79			

D. Monthly and Annual Energy or Fuel Savings

No cost data are available on fuel savings.

E. Energy and Mass Balances

Figure 6 is a daily record for September 25, 1977 of the cooling system performance using the Rankine cycle unit. This was a clear day, and no auxiliary energy was used. The peak solar flux was 1070 w/m^2, and the maximum collector outlet temperature was 104°C. The changeover from cooling from storage to cooling with the chiller can be seen to occur around noon (Mode 5 to Mode 3). The energy flow into the tank during chiller operation is due to excess chilled water being stored because the chiller output exceeds the building cooling load.

Appendix A contains daily energy summaries for the entire heating season.

III. SYSTEM ECONOMIC ANALYSIS

A. Total Cost of the Solar Portion of the System

The total add-on cost of the solar energy system (excluding experimental equipment) was $440,000. Of this figure, $135,000 was for collectors. The total cost of the building was $4,600,000, including engineering. No operating cost figures are available.

H. User Reactions and Comments

The system has performed reliably, providing occupant comfort within normal standards. Several control system modifications were made to obtain more effective use of cold storage, and data for a full cooling season have not yet been accumulated.

SUBSYSTEM PERFORMANCE

A. SOLAR COLLECTORS

1. Description of Physical Configuration

A general description of the collector is given in Section I.C.2. Each .61 m by 3.05 m collector combines the functions of roof and solar collector by providing weather exclusion, structural support, thermal insulation, and energy collection.

The collectors achieve good thermal performance through the use of single-pane, high transmission, .318 cm-thick tempered plate glass glazing and an absorber surface which has been electroplated with highly selective black chrome to minimize heat loss by radiation. The absorber plate and all structural elements of the collector are fabricated from mild steel for strength and economy. The coolant passages are formed by seam-welding the edges of two steel plates together, intermittently spot-welding the surface, and expanding the assembly under pressure to give a quilted surface appearance. A cutaway drawing of a collector is shown in Figure 7.

Individual collectors are bolted to 20.3 cm roof purlin beams and are connected to the structural support in a manner which allows for thermal expansion.

2. Thermal Performance Characteristics

A collector efficiency plot is given in Figure 3. Data are shown from actual instantaneous operating points. The solid line was obtained from experimental test data on the collector.

Under actual operating conditions, collector flow rate is around 29.0 l/sec of water equivalent at 15.6°C. Total pressure drop in the system, including all pipes and the heat exchanger, is 96.5 kPa. Pumping power for the oil coolant is 9.6 kw.

3. Lifetime Performance Characteristics

No leakage has been detected. One glass cover was broken during installation, but no other breakage has occurred. Corrosion is not expected to occur due to the use of the oil coolant.

B. HEAT TRANSFER SUBSYSTEM

1. Description of Physical Configuration

Collected heat is transferred from the oil to water via a shell and tube heat exchanger.

2. Thermal Performance Characteristics

Typical values of heat exchanger variables in the heating mode are given below:

	Oil Side	Water Side
Inlet Temperature, °C	75.2	57.3
Outlet Temperature, °C	69.4	61.6
Flow (water at 15.6°C), lb/sec	29.0	19.5
Pump Power, kw	9.6	1.1

C. THERMAL ENERGY STORAGE SUBSYSTEM

1. Description of Physical Configuration

The two tanks are 38 m^3 and 19 m^3 in volume as described previously. The larger tank is 7.9 m high to promote stratification.

2. Thermal Performance Characteristics

The temperature of the equipment room averages about 18.3°C in the winter and 26.7°C in the summer. The loss coefficient of the tank is .81 $W/m^2°C$. The normal maximum temperatures for hot water storage in the large and small tank are 82°C and 104°C, respectively. The normal minimum temperature for cold storage is 9°C.

In the heating mode, hot water flow out of the large tank varies depending upon heating demand at the terminal boxes, but is nominally 3.8 l/sec (18.3°C water). Pumping power for hot water is 1.2 kw. In the cooling mode, cold water flow from the large tank is 12.6 l/sec, and hot water flow to the chiller from the small tank is 22.1 l/sec. Pumping power in the cooling mode was not measured for the period of operation reported.

D. AIR CONDITIONING SUBSYSTEM

1. Description of Physical Configuration

Either of the two water chillers can be used. The absorption unit is a York model ESIA2, derated to 229 kw with 85°C water. The Rankine cycle unit is an experimental unit designed by Barber-Nichols with a design point of 271 kw with 93°C. Both units have a COP of 0.75 under design conditions. Heat rejection is through a 31.6 l/sec cooling tower.

2. Thermal Performance Characteristics

A performance summary of the two cooling units is given in Figure 9. Carnot COP is defined as

$$\text{Carnot COP} = \frac{T_{hw} - T_{cw}}{T_{hw}} \times \frac{T_{chw}}{T_{cw} - T_{chw}}$$

T_{hw} = Hot water inlet temperature, °K

T_{cw} = Condenser water inlet temperature, °K

T_{chw} = Chilled water outlet temperature, °K

Fig. 1

E DIVISION ENGINEERING DATA SHEET

	REQUESTING GROUP:	JO. NO.:	
BY:	REQUESTED BY:	SHEET:	OF:
TITLE:			
DESCRIPTION:			

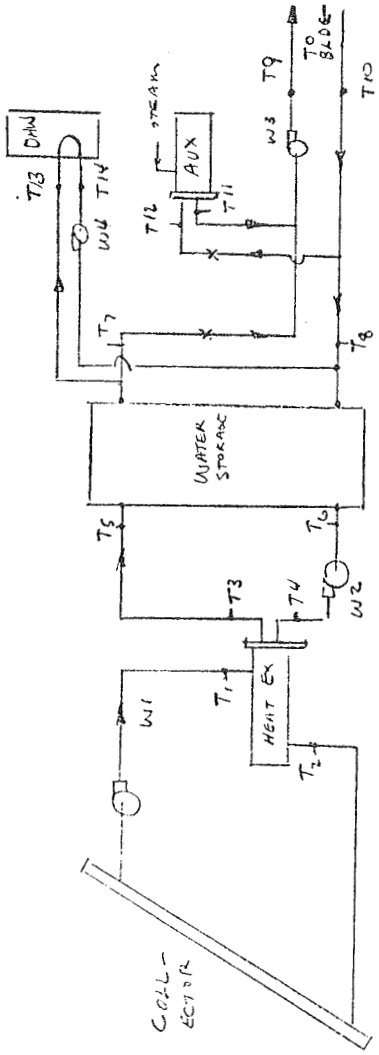

FIG 1 STUDY CENTER SOLAR HEATING SYSTEM

Figure 2 NSRSC Collector

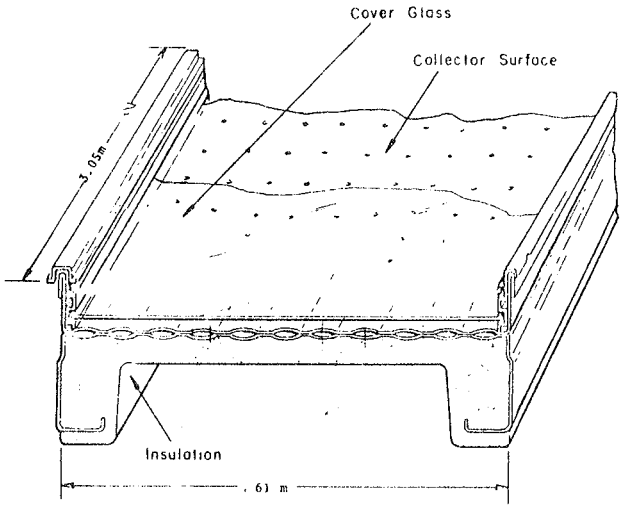

Cutaway Of
Structurally Integrated Solar Collector Unit

Fig. 3. SIDE-BY-SIDE COLLECTOR TEST
LASL STUDY CENTER COLLECTORS
1/20/77 to 3/6/77